https://doi.org/10.5194/acp-2019-1211
Preprint. Discussion started: 21 January 2020

Atmospheric Chemistry and Physics Discussions

Historical and future changes in air pollutants from CMIP6 models

Steven T. Turnock[1], Robert J. Allen[2], Martin Andrews[1], Susanne E. Bauer[3,4], Louisa Emmons[5], Peter Good[1], Larry Horowitz[6], Martine Michou[7], Pierre Nabat[7], Vaishali Naik[6], David Neubauer[8], Fiona M. O'Connor[1], Dirk Olivié[9], Michael Schulz[9], Alistair Sellar[1], Toshihiko Takemura[10], Simone Tilmes[5], Kostas Tsigaridis[3,4], Tongwen Wu[11], Jie Zhang[11]

[1]Met Office Hadley Centre, Exeter, UK
[2]Department of Earth and Planetary Sciences, University of California Riverside, Riverside, California, USA
[3]Center for Climate Systems Research, Columbia University, New York, NY, USA
[4]NASA Goddard Institute for Space Studies, New York, NY, USA
[5]Atmospheric Chemistry Observations and Modelling Lab, National Center for Atmospheric Research, Boulder, CO, USA
[6]DOC/NOAA/OAR/Geophysical Fluid Dynamics Laboratory. Biogeochemistry, Atmospheric Chemistry, and Ecology Division, Princeton, USA
[7]Centre National de Recherches Météorologiques (CNRM), Université de Toulouse, Météo-France, CNRS, Toulouse, France
[8]Institute of Atmospheric and Climate Science, ETH Zurich, Zurich, Switzerland
[9]Division for Climate Modelling and Air Pollution, Norwegian Meteorological Institute, Oslo, Norway
[10]Research Institute for Applied Mechanics, Kyushu University, Fukuoka, Japan
[11]Beijing Climate Center, China Meteorological Administration, Beijing, China

Correspondence to: Steven Turnock (steven.turnock@metoffice.gov.uk)

Abstract.

Poor air quality is currently responsible for large impacts on human health across the world. In addition, the air pollutants, ozone (O_3) and particulate matter less than 2.5 microns in diameter ($PM_{2.5}$), are also radiatively active in the atmosphere and can influence Earth's climate. It is important to understand the effect of air quality and climate mitigation measures over the historical period and in different future scenarios to ascertain any impacts from air pollutants on both climate and human health. The 6th Coupled Model Intercomparison Project (CMIP6) presents an opportunity to analyse the change in air pollutants simulated by the current generation of climate and Earth system models that include a representation of chemistry and aerosols (particulate matter). The shared socio-economic pathways (SSPs) used within CMIP6 encompass a wide range of trajectories in precursor emissions and climate change, allowing for an improved analysis of future changes to air pollutants. Firstly, we conduct an evaluation of the available CMIP6 models against surface observations of O_3 and $PM_{2.5}$. CMIP6 models show a consistent overestimation of observed surface O_3 concentrations across most regions and in most seasons, with a large diversity in simulated values over northern hemisphere continental regions. Conversely, observed surface $PM_{2.5}$ concentrations are consistently underestimated by CMIP6 models, particularly for the northern hemisphere winter months, with the largest model diversity near natural emission source regions. Over the historical period (1850-2014) large increases in both surface O_3 and $PM_{2.5}$ are simulated by the CMIP6 models across all regions, particularly over the mid to late 20th Century when anthropogenic emissions increase markedly. Large regional historical changes are simulated for both pollutants, across East and South Asia, with an increase of up to 40 ppb for O_3 and 12 μg m^{-3} for $PM_{2.5}$. In future scenarios containing strong air quality and climate mitigation measures (ssp126), air pollutants are substantially reduced across all regions by up to 15 ppb for O_3 and 12 μg m^{-3} for $PM_{2.5}$. However, for scenarios that encompass weak action on mitigating climate and reducing air pollutant emissions (ssp370), increases of both surface O_3 (up 10 ppb) and $PM_{2.5}$ (up to 8 μg m^{-3}) are simulated across most regions. Although, for regions like North America and Europe small reductions in $PM_{2.5}$ are simulated in this scenario. A comparison of simulated regional changes in both surface O_3 and $PM_{2.5}$ from individual CMIP6 models highlights important differences due to the interaction of aerosols, chemistry, climate and natural emission sources within models. The prediction of regional air pollutant concentrations from the latest climate and Earth system models used within CMIP6 shows that the particular future trajectory of climate and air quality mitigation measures could have important consequences for regional air quality, human health and near-term climate. Differences between individual models emphasises the importance of understanding how future Earth system feedbacks influence natural emission sources.

https://doi.org/10.5194/acp-2019-1211
Preprint. Discussion started: 21 January 2020

Atmospheric Chemistry and Physics Discussions

1 Introduction

Air pollutants are important atmospheric constituents as they have large impacts on human health (Lelieveld et al., 2015), damage ecosystems (Fowler et al., 2009) and can also influence climate through changes in the Earth's radiative balance (Boucher et al., 2013; Myhre et al., 2013). Two major components of air pollution at the surface are ozone (O_3) and particulate matter less than 2.5 microns in diameter ($PM_{2.5}$). Exposure to present day ambient concentrations of these two air pollutants was estimated as causing up to 4 million premature deaths per year (Apte et al., 2015; Malley et al., 2017). Over recent decades, the impact on human health from exposure to air pollutants has been increasing (Butt et al., 2017; Cohen et al., 2017). Additionally, elevated levels of air pollutants over recent decades have also been responsible for ecosystem damage to crops and vegetation, although there have been recent improvements in environmental health (de Wit et al., 2015).

In terms of climate impact, tropospheric O_3 has a positive radiative forcing on climate over the industrial period and is the third most important greenhouse gas in terms of radiative forcing (Myhre et al., 2013). However, depletion of O_3 in the stratosphere has resulted in a net negative top of atmosphere radiative forcing over recent decades (Checa-Garcia et al., 2018). Particulate matter (PM), also referred to as aerosols, has an overall negative radiative forcing on climate, both directly and indirectly through the modification of cloud properties (Boucher et al., 2013). Both O_3 and PM are relatively short lived in the troposphere, with a typical lifetime of less than 2 weeks in the lower atmosphere, and are commonly referred to as Near Term Climate Forcers (NTCFs). Future air pollutant concentrations and distributions are driven by changes to both precursor emissions and climate. Emission control measures on a national and international level can both influence future changes to air pollutants, with global increases in CH_4 abundance potentially offsetting benefits to surface O_3 from local emission reductions (Wild et al., 2012). For $PM_{2.5}$, changes in concentrations are dependent on both emission rates and levels of atmospheric oxidants, although changes in specific aerosol components can be more directly related to emissions, e.g. black carbon. In a warming world, background O_3 concentrations over remote locations are likely to decrease (Isaksen et al., 2009; Fiore et al., 2012; Doherty et al., 2013), whereas over anthropogenic source regions, which have higher baseline surface O_3 concentrations, an increase is anticipated (Rasmussen et al., 2013; Colette et al., 2015). The climate impact on $PM_{2.5}$ is much more uncertain and variable across regions, with both increases and decreases predicted due to the uncertainty of future meteorological effects (Jacob and Winner, 2009; Allen et al., 2016; Shen et al., 2017). However, any such climate change impacts on $PM_{2.5}$ are considered to be smaller than the effect from implementing emission mitigation measures (Westervelt et al., 2016).

Experiments conducted as part of the 5th Coupled Model Intercomparison Project (CMIP5; Taylor et al., 2012) and the Atmospheric Chemistry and Climate Model Intercomparison Project (ACCMIP, Lamarque et al., 2013) contributed to a multi-model assessment of future trends in air pollutants. Global annual mean surface O_3 concentrations were predicted to increase by up to 5 ppb in 2100 using RCP8.5 (Representative Concentration Pathway with an anthropogenic radiative forcing of 8.5 W m^{-2} in 2100); the RCP with largest increases in methane (CH_4) abundances and the largest climate change signal used in CMIP5 (Kirtman et al., 2013). The other RCPs used in CMIP5 had a lower climate forcing and smaller changes in CH_4 abundance with models predicting global annual mean surface O_3 concentrations that showed little change in the short term (up to 2050) but decreased by around 5 ppb in 2100. The scenario differences in the global mean response for surface O_3 were generally reflected across other regions, although with a larger magnitude of change over the northern hemisphere continental regions. The predicted range of future surface O_3 concentrations was previously found to be dominated by changes in precursor emissions (Fiore et al., 2012). However, in regions remote from pollution sources (low-NOx) future climate change was shown to result in a small reduction in surface O_3 concentrations. For $PM_{2.5}$, results from CMIP5 and ACCMIP models showed annual mean concentrations declining in most regions and across all scenarios due to the reduction in aerosol emissions. Globally, $PM_{2.5}$ concentrations reduced by ~1 μg m^{-3} by 2100, whereas larger regional reductions of up to 6 μg m^{-3} were predicted by 2100. Exceptions to this occurred over South and East Asia where $PM_{2.5}$ concentrations increased by up to 3 μg m^{-3} in the near-term (up to 2050), after which concentrations reduced by 2100. The largest difference in the response of $PM_{2.5}$ across the

https://doi.org/10.5194/acp-2019-1211
Preprint. Discussion started: 21 January 2020

scenarios was also shown across East and South Asia due to differences in the carbonaceous and sulphur dioxide (SO_2) emission trajectories (Fiore et al., 2012). Future $PM_{2.5}$ concentrations over Africa and the Middle East were shown to be quite noisy due to the large meteorological variability that influences dust emissions over these regions.

The current set of experiments conducted for the 6th Coupled Model Intercomparison Project (CMIP6; Eyring et al., 2016) represent an opportunity to update the assessment of current and future levels of air pollutants using the latest generation of Earth system and climate models. A new set of future scenarios have been generated for CMIP6, the Shared Socio-economic Pathways (SSPs), which combine different trends in social, economic and environmental developments (O'Neill et al., 2014). Varying amounts of emission mitigation to NTCFs are applied on top of the baseline social and economic developments to meet predefined climate and air quality targets in the future, allowing for a wider range of future air pollutant trajectories to be assessed than occurred in CMIP5 (Rao et al., 2017; Riahi et al., 2017). Initial assessments have been made of future changes to air pollutants in the SSPs using simplified models. The sustainability pathway (SSP1) leads to improvements in both air quality and climate, whereas SSP3 (regional rivalry) is not compatible with achieving air quality and climate goals, and the conventional fuels (SSP5) pathway improves air quality at the expenses of climate (Reis et al., 2018). Strong climate and air pollutant mitigation measures in SSP1 were shown to reduce global annual mean surface O_3 concentrations by more than 3.5 ppb, whereas for SSP3 O_3 concentrations over Asia were predicted to increase by 6 ppb (Turnock et al., 2019). These studies highlighted the potential large regional variability in the response of air pollutants to the different assumptions in the future pathways and also the need for a full model assessment using the current generation of Earth System Models (ESMs) that take into account both changes in emissions and climate.

In this study, we use results from experiments conducted as part of CMIP6 to make a first assessment of historical and future changes in air pollutants. First, we assess the performance of CMIP6 models in simulating present day air pollutants by conducting an evaluation against observations of O_3 and $PM_{2.5}$. Regional changes in surface O_3 and $PM_{2.5}$ are computed over the historical period (1850-2014) to provide context with future changes. We are then able to show future projections of air pollutants over different world regions under different Shared Socio-economic Pathways (SSPs) used in the CMIP6 experiments. Finally, a comparison is made of individual CMIP6 models for a single future scenario to identify potential reasons for model discrepancies.

2 Methods

2.1 Air Pollutant Emissions

A new set of historical and future anthropogenic air pollutant emissions has been developed and used as part of CMIP6. The historical anthropogenic emissions are from the Community Emissions Data System (CEDS) and a new dataset was developed for biomass burning emissions, both of which provides information on emissions from 1750 to 2014 (van Marle et al., 2017; Hoesly et al., 2018). The SSPs used in future CMIP6 experiments represent an update from the RCPs used in CMIP5, as they combine pathways of socio-economic development with targets to achieve a certain level of climate mitigation (O'Neill et al., 2014; van Vuuren et al., 2014; Riahi et al., 2017). The SSPs are divided into the following 5 different pathways depending on their social, economic and environmental development: SSP1 – sustainability, SSP2 - middle-of-the-road, SSP3 – regional rivalry, SSP4 - inequality, SSP5 – fossil fuel development. An assumption about the degree of air pollution control (strong, medium or weak) is included on top of the baseline pathway, with stricter air pollution controls assumed to be tied to economic development (Rao et al., 2016). Weak air pollution controls occur in SSP3 and SSP4, with medium controls in SSP2 and strong air pollution controls in SSP1 and SSP5 (Gidden et al., 2019). A particular climate mitigation target, in terms of an anthropogenic radiative forcing by 2100, is included on top of each SSP and is achieved using a range of emissions mitigation measures appropriate to each SSP. Climate mitigation targets vary from a weak mitigation scenario with an anthropogenic radiative forcing of 8.5 W m^{-2} by 2100, comparable with a 5 °C temperature change (Riahi et al., 2017), to a strong mitigation

https://doi.org/10.5194/acp-2019-1211
Preprint. Discussion started: 21 January 2020

Atmospheric Chemistry and Physics Discussions

scenario with a radiative forcing of 1.9 W m^{-2} by 2100, in accordance with the Paris agreement for keeping temperatures below 2 °C (United Nations, 2016). Some climate mitigation targets are comparable with those of the RCPs used in CMIP5 (2.6, 4.5 and 6.0), whilst others are new, e.g. ssp534 is included as a delayed mitigation scenario. A scenario specific to the Aerosol and Chemistry Model Intercomparison Project (AerChemMIP), ssp370-lowNTCF, is also included to study the impact of mitigation measures to specifically control NTCFs on top of ssp370. Future biomass burning emissions vary in each scenario, depending on the particular land-use assumptions (Rao et al., 2017). Whilst future anthropogenic and biomass burning emissions are prescribed in each CMIP6 model from the same dataset, other natural emissions, e.g. dust, biogenic volatile organic compounds (BVOCs) etc., will be different and depend on the individual model configuration.

Figure 1 shows the future changes in global total (anthropogenic and biomass) emissions of the major air pollutant precursors across all of the CMIP6 scenarios, provided as input to the CMIP6 models. The overlying feature is that global air pollutant emissions are predicted to reduce across the majority of scenarios by 2100. The exception to this is that global and regional emissions increase or remain at present day levels for ssp370 (Fig. 1 and Fig. 2). Some air pollutant emissions increase in the near-term in other scenarios e.g. nitrogen oxides (NOx) in ssp585, but by 2100 these have been reduced. Future CH_4 abundances show the largest diversity amongst the SSPs. Large increases in global CH_4 abundances of more than 50% are predicted for the fossil fuel dominated pathways of ssp370 and ssp585, whereas large reductions are predicted to occur in the strong mitigation scenarios of SSP1.

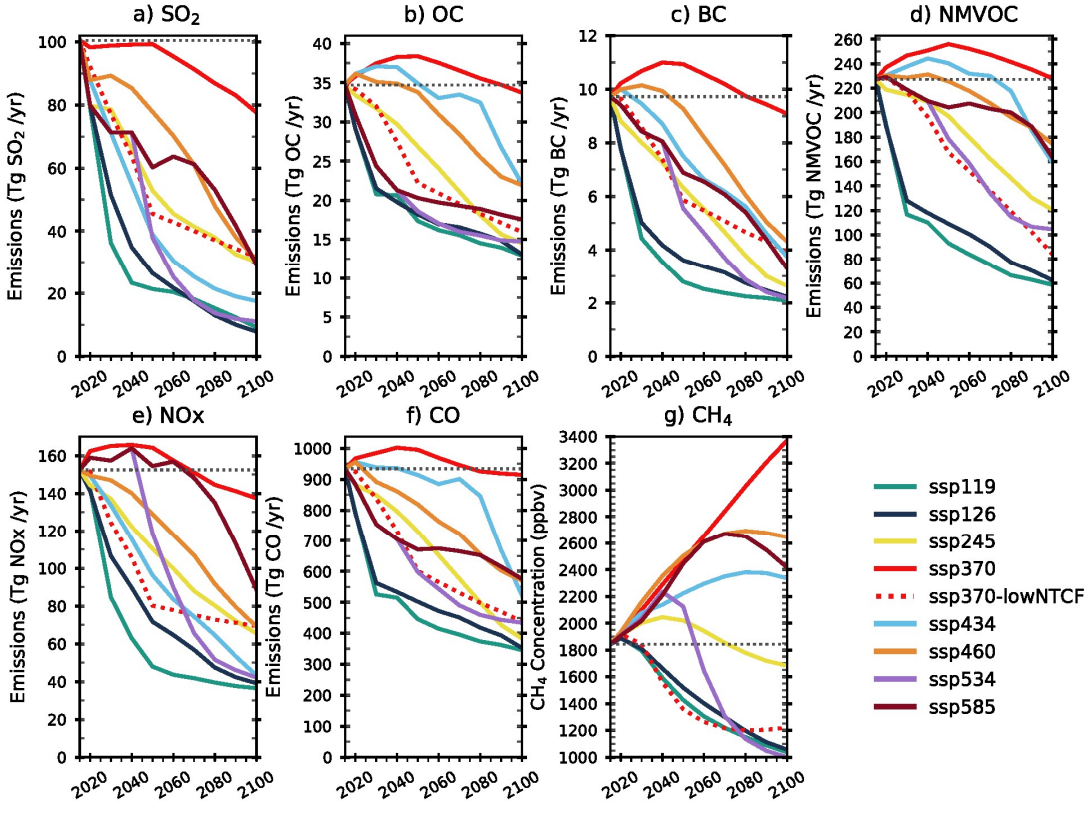

Figure 1: Changes in annual total (anthropogenic and biomass) global air pollutant emissions (relative to 2015) of sulphur dioxide (SO_2), organic carbon (OC), black carbon (BC), non-methane volatile organic compounds (NMVOCs), nitrogen oxides (NOx), carbon monoxide (CO) and global methane (CH_4) abundances in the future CMIP6 scenarios used as input to CMIP6 models. The dashed black line represents the 2015 value.

For SO_2, large reductions of more than 50% are shown for most scenarios and across most regions (Figure 2), apart from Africa and Asia in ssp370. Near-term (2050) increases in SO_2 occur over South Asia and other developing regions, which are then

https://doi.org/10.5194/acp-2019-1211
Preprint. Discussion started: 21 January 2020

Atmospheric Chemistry and Physics Discussions

reduced in the latter half of the 21st Century. Over Europe and North America consistent decreases are predicted across all scenarios. The other major aerosol emissions, OC and BC, show similar reductions to SO_2 across all scenarios and regions. For all aerosol and aerosol precursors, a reduction of 80-100% (relative to 2015) in regional emissions is predicted by 2100 in the strong mitigation scenarios. Changes in the emissions of the O_3 precursors, NOx, CO and NMVOCs, show a similar increase across most regions for ssp370 but a general decrease in other scenarios. The change in these emissions are particular diverse across all the scenarios in South Asia with large relative increases in ssp370, contrary to the large decreases in ssp126. Across East Asia there is an increase in NOx emissions for ssp370 in 2050 but a long term reduction across all scenarios.

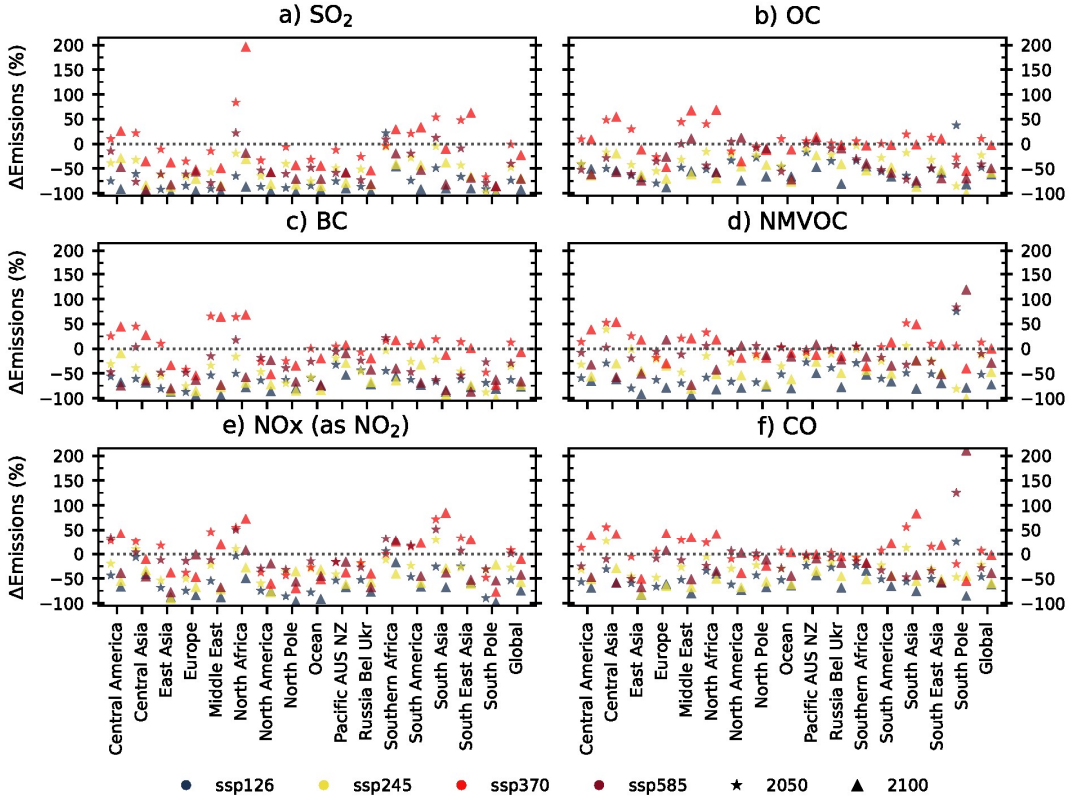

Figure 2: Percent change in 2050 (stars) and 2100 (triangles), relative to 2015, for annual mean total (anthropogenic and biomass) air pollutant emissions of SO_2, OC, BC, NMVOCs, NOx and CO across different world regions in the 4 Tier 1 future CMIP6 scenarios. Regions are defined in Figure S1.

2.2 CMIP6 Simulations

Surface concentrations of O_3 and $PM_{2.5}$ have been obtained from all the CMIP6 models that made appropriate data available on the Earth System Grid Federation (ESGF) at the time of writing. To study changes in surface air pollutants over the industrial period data has been obtained from the coupled historical simulations (Eyring et al., 2016) over the period 1850 to 2014 from all of the available ensemble members of each available CMIP6 model. For each model, a mean is taken using all available ensemble members prior to the calculation of multi-model mean. For model evaluation purposes, 10 years of data from historical simulations has been used over the period that is relevant to the particular observational dataset (2000-2010 for ground-based $PM_{2.5}$, 2004-2014 for $PM_{2.5}$ reanalysis product and 2005-2014 for ground-based O_3). To investigate future changes in air pollutants, all available data has been obtained over the period 2015 to 2100 for each of the different future coupled atmosphere-ocean model experiments, conducted as part of ScenarioMIP (O'Neill et al., 2016). CMIP6 model data

https://doi.org/10.5194/acp-2019-1211
Preprint. Discussion started: 21 January 2020

Atmospheric Chemistry and Physics Discussions

has also been obtained for the AerChemMIP specific ssp370-lowNTCF scenario, which was only required to be conducted over the period 2015-2055 (Collins et al., 2017).

Concentrations of both pollutants at the surface have been obtained by extracting the lowest vertical level of the full 3D field output on the native horizontal and vertical grid of each model (the "AERmon" CMIP6 table ID). For O_3, this is supplied as a separate diagnostic which can be used directly. However, models contributing to CMIP6 will not all directly output $PM_{2.5}$ and the calculation of $PM_{2.5}$ will not be consistent across individual models due to the different treatment of aerosols and their components. For example only a few CMIP6 models include the simulation of ammonium nitrate in their aerosol scheme (currently, only GISS-E2-1-H and GFDL-ESM4 have provided nitrate mass mixing ratios on the ESGF database). Therefore it has been necessary to use a definition of $PM_{2.5}$, which is consistent across all models and is calculated offline. In this study surface $PM_{2.5}$ is defined as the sum of the individual dry aerosol mass mixing ratios of black carbon (BC), total organic aerosol (OA – both primary and secondary sources), sulphate (SO_4), sea salt (SS) and dust (DU) from the lowest model level extract of the full 3D model fields. All BC, OA and SO_4 aerosol mass is assumed to be present in the fine size fraction (< 2.5 μm), whereas a factor of 0.25 for SS and 0.1 for DU has been used to calculate the approximate contribution from these components to the fine aerosol size fraction (Eq. 1).

$$PM_{2.5} = BC + OA + SO_4 + (0.25 \times SS) + (0.1 \times DU) \quad (1)$$

The factors used to calculate the contribution of SS and DU concentrations to the $PM_{2.5}$ size fraction are likely to depend on the individual aerosol scheme and the simulated aerosol size distribution within a particular model. The calculation of an approximate $PM_{2.5}$ concentration using Eq. (1) is therefore likely to introduce some errors but it does provide an estimate that is consistent across models and also with that previously used in CMIP5 and ACCMIP (Fiore et al., 2012; Silva et al., 2013, 2017). For the CNRM-ESM2-1 model, anomalously large concentrations were obtained from the sea salt mass mixing ratios. Sensitivity tests with this model suggested that a much smaller factor of 0.01 was more appropriate to use for SS, which takes into account the non-dry nature of the sea salt aerosols and the large possible size range, up to 20 μm in diameter, of sea salt particles within the CNRM-ESM2-1 model (P Nabat 2019, personal communication, 27th November).

Details of the data used in this study from different CMIP6 models, in both the historical and future scenarios, is presented below in Table 1. For the historical period, data was available from 5 different CMIP6 models for O_3 and 10 models for $PM_{2.5}$. The future scenario with the most data available was ssp370, with 4 models suppling data for O_3 and 7 models for $PM_{2.5}$. For the other Tier 1 CMIP6 scenarios (ssp126, ssp245 and ssp585), data was only available for 2 models for O_3 and 4 for $PM_{2.5}$ (all components). It was decided to focus the analysis on ssp370 and other Tier 1 scenarios due to the limited availability of model data for Tier 2 scenarios (ssp119, ssp434, ssp460 and ssp534). The results from an O_3 parameterisation (Turnock et al., 2018, 2019) has also been included in the analysis of surface O_3 from CMIP6 models for both the historical and future scenarios and is referred to in this study as HTAP_param. The O_3 parameterisation does not take into account the effects of climate change on surface O_3 concentrations and therefore provides an estimate of the emission-only driven changes to surface O_3 with which to compare to the climate and Earth System models.

https://doi.org/10.5194/acp-2019-1211
Preprint. Discussion started: 21 January 2020

Atmospheric Chemistry and Physics Discussions

210 **Table 1 –Number of ensemble members used for the historical and future scenarios experiments from each model in the analysis of surface O_3 and $PM_{2.5}$ in this study**

Model	Pollutant	historical	ssp126	ssp245	ssp370	ssp370-lowNTCF	ssp585	Model Refs	Data Citation
BCC-ESM1	O_3, $PM_{2.5}$	3			3	3		(Wu et al., 2019a, 2019b)	(Zhang et al., 2018, 2019)
CESM2-WACCM	O_3, $PM_{2.5}$	3			1	1		(Emmons et al., 2019; Gettelman et al., 2019; Tilmes et al., 2019)	(Danabasoglu, 2019a, 2019b, 2019c)
CNRM-ESM2-1	$PM_{2.5}$	3			3	3		(Séférian et al., 2019)	(Seferian, 2018, 2019; Voldoire, 2019)
GFDL-ESM4	O_3, $PM_{2.5}$	1	1	1	1	1	1	(Dunne, 2019; Horowitz, 2019)	(Horowitz et al., 2018; John et al., 2018; Krasting et al., 2018)
HadGEM3-GC31-LL	$PM_{2.5}$	4	1	1			1	(Kuhlbrodt et al., 2018)	(Ridley et al., 2018; Good, 2019)
MIROC6 - ES2L	$PM_{2.5}$	3	1	1	1		1	(Takemura, 2012; Hajima et al., 2019)	(Hajima and Kawamiya, 2019; Tachiiri and Kawamiya, 2019)
MPI-ESM1.2-HAM	$PM_{2.5}$	1			1	1		(Tegen et al., 2019)	(Neubauer et al., 2019)
GISS-E2-1-H	O_3, $PM_{2.5}$	5 2						(Bauer and Tsigaridis, 2019)	(NASA Goddard Institute For Space Studies (NASA/GISS), 2018)
NorESM2-LM	$PM_{2.5}$	1						(Karset et al., 2018; Kirkevåg et al., 2018)	(Norwegian Climate Center (NCC), 2018)
UKESM1-0-LL	O_3, $PM_{2.5}$	5	5	5	5		5	(Sellar et al., 2019)	(Good et al., 2019; Tang et al., 2019)
Total Number of models	O_3	5	2	2	4	3	2		
	$PM_{2.5}$	10	4	4	7	4	4		

https://doi.org/10.5194/acp-2019-1211
Preprint. Discussion started: 21 January 2020

Atmospheric Chemistry and Physics Discussions

2.3 Surface Observations

Present day surface O_3 and $PM_{2.5}$ simulated by all of the CMIP6 models is evaluated against surface observations to ascertain model biases and inter-model discrepancies. Surface O_3 observations are obtained from the database of the Tropospheric Ozone Assessment Report (TOAR) (Schultz et al., 2017). The TOAR database provides a gridded product of surface O_3 observations over the period 1970 to 2015. The majority of measurement sites are located in North America and Europe, with a smaller number of other sites in East Asia, Australia, New Zealand, South America, Southern Africa, Antarctica and remote ocean locations. Here we compile a monthly mean climatology of all available O_3 observations over the period 2005-2014 from measurement locations that are classified as rural in the TOAR database (Schultz et al., 2017). The rural locations were selected to be representative of background (i.e. non-urban) O_3 concentrations and are considered to be more appropriate in evaluating the simulated values obtained at the relatively coarse horizontal resolution of the global ESMs. Simulated surface O_3 concentrations from the CMIP6 models are re-gridded onto the same resolution of the observational product (2° x 2°) for evaluation purposes.

Surface $PM_{2.5}$ observations have been obtained from all of the locations compiled in the database of the Global Aerosol Synthesis and Science Project (GASSP: http://gassp.org.uk/data/, Reddington et al., 2017) to evaluate CMIP6 models. Background, non-urban, $PM_{2.5}$ data is compiled in the GASSP database from three major networks: the Interagency Monitoring of Protected Visual Environments (IMPROVE) network in North America, the European Monitoring and Evaluation Programme (EMEP) and Asia-Pacific Aerosol Database (A-PAD). Again, like for O_3, the networks/observations for $PM_{2.5}$ were selected to be representative of non-urban environments, which are more appropriate for the evaluation of global ESMs. With the exception of the IMPROVE network, most measurements of $PM_{2.5}$ began after the year 2000. Like for O_3, we compile a monthly mean climatology of $PM_{2.5}$ but now over the period of 2000 to 2010, selected as the GASSP database contained the most observations within this period. Simulated surface $PM_{2.5}$ was computed from CMIP6 models over the same time period as the observations and linearly interpolated to each measurement location. Whilst the surface observations measure total $PM_{2.5}$ mass, the computed $PM_{2.5}$ from CMIP6 models use Eq. 1 and does not include all observable $PM_{2.5}$ aerosol components (e.g. nitrate aerosol). Therefore it is anticipated that the CMIP6 models will underrepresent the $PM_{2.5}$ observations in this comparison.

To address the anticipated disparity between the observed ground based $PM_{2.5}$ and the approximate $PM_{2.5}$ from CMIP6 models, a further comparison has been made between the CMIP6 models and the Modern-Era Retrospective Analysis for Research and Applications, version 2 (MERRA-2), aerosol reanalysis product (Buchard et al., 2017; Randles et al., 2017). The MERRA-2 aerosol product assimilates observations of Aerosol Optical Depth (AOD) from ground based and satellite remote sensing platforms into model simulations that use the GEOS-5 atmospheric model coupled to the GOCART aerosol module. The data assimilation used in MERRA-2 generally improves comparisons of $PM_{2.5}$ with observations but there are still overestimations due to dust and sea salt and underestimations over East Asia (Buchard et al., 2017; Provençal et al., 2017). Separate mass mixing ratios for BC, OA, SO_4, SS and DU aerosol components are provided from MERRA-2, which are then combined using

https://doi.org/10.5194/acp-2019-1211
Preprint. Discussion started: 21 January 2020

Atmospheric Chemistry and Physics Discussions

the formula in Eq. 1 to make an approximate $PM_{2.5}$. Monthly mean approximate $PM_{2.5}$ concentrations are then computed over the period 2005-2014 from the MERRA-2 reanalysis product to provide a more direct comparison and enhanced spatial coverage against the approximate $PM_{2.5}$ concentrations calculated from the CMIP6 models calculated over the same time period.

3 Present-day Model Evaluation of Air Pollutants

3.1 Surface Ozone

The 5 CMIP6 models with data available for the historical experiments are evaluated against surface O_3 observations from the TOAR database over the period 2005-2014. A long-term evaluation of surface O_3 concentrations from CMIP6 models using observations compiled over the 20th Century is presented separately in Griffiths et al., (2019). Figure 3 shows the seasonal multi-model mean in surface O_3 over the period 2005-2014 and the standard deviation across the 5 CMIP6 models. The seasonal mean surface O_3 concentrations and evaluation against observations for individual CMIP6 models are shown in Figures S2–S6. Higher surface O_3 concentrations are simulated in the northern hemisphere summer (June, July, August- JJA) when O_3 formation is enhanced by increased photolytic activity and levels of oxidants, as well as larger biogenic emissions. The hemispheric difference in surface O_3 is smaller in December, January and February (DJF) when O_3 production is less in the northern hemisphere but higher in the southern hemisphere. However, model diversity is larger in DJF (Fig. 3b) due to individual models simulating different seasonal cycles of O_3, particularly UKESM1 which has the most pronounced seasonal cycle of all 5 models (Fig. S2).

The multi-model mean of CMIP6 models overestimates surface O_3 concentrations in both seasons when compared to observations from the TOAR database, although they do capture the broad hemispheric gradient in O_3 concentrations (Fig. 3c and 3f). These results are consistent with the previous evaluation of ACCMIP models (Young et al., 2018). The overestimation in the CMIP6 models analysed here could be due to the coarse resolution of the ESMs, an excess of O_3 chemical production (potentially due to an overabundance of NOx and/or VOCs) and weak O_3 deposition. Smaller model biases exist in DJF (<5 ppb) than in JJA (5-15 ppb), mostly attributed to the strong seasonal cycle simulated by UKESM1. In contrast to other models (Fig. S2 – S6), UKESM1 underpredicts surface O_3 in DJF over most continental northern hemisphere locations, potentially indicating there is excessive NOx titration of O_3 in this model.

https://doi.org/10.5194/acp-2019-1211
Preprint. Discussion started: 21 January 2020

Atmospheric Chemistry and Physics Discussions

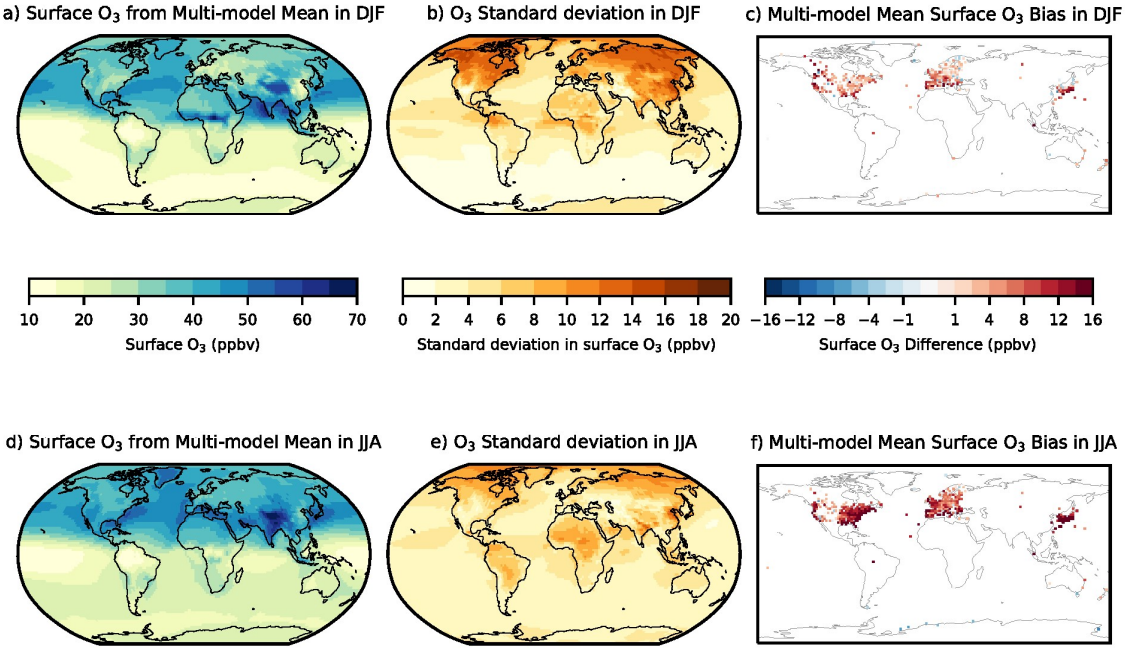

Figure 3 – Multi-model (5 CMIP6 models) seasonal mean surface O_3 concentrations in a) December January, February (DJF) and d) June, July, August (JJA) over the 2005-2014 period. The standard deviation in the multi-model mean in b) DJF and e) JJA. The difference between the multi-model mean and TOAR observations in c) DJF and f) JJA.

The observed annual cycle in surface O_3 averaged across measurement locations within different regions is compared to that simulated by CMIP6 models (Figure 4). Across most regions, the mean annual cycle from CMIP6 models compares relatively well to that observed. The overprediction of surface O_3 values in JJA is evident across most regions, as is the strong seasonal cycle in UKESM1 for northern hemisphere continental regions. Additionally, the timing of peak O_3 over continental northern hemisphere locations occurs earlier in the observations (springtime) than in the CMIP6 models (spring and summer), which is consistent with that from ACCMIP models (Young et al., 2018). At oceanic observation locations there is also a consistent overestimate of surface O_3 by CMIP6 models across all seasons, indicating that O_3 deposition rate could be underestimated here. There is also a large overestimation (~20 ppb) in all models at the one observation location in South East Asia, potentially due to difficulty in simulating O_3 in the maritime continental boundary layer using lower resolution global ESMs. In contrast to this, CMIP6 models tend to underpredict the observed surface O_3 concentrations at locations in the South Pole region in JJA by ~5 ppb. This could be due to lack of long range transport of O_3 to these sites, inaccuracies in southern hemisphere precursor emissions, or because of the difficulty in simulating O_3 concentrations at the appropriate elevation of measurement sites located on the Antarctic ice sheet.

https://doi.org/10.5194/acp-2019-1211
Preprint. Discussion started: 21 January 2020

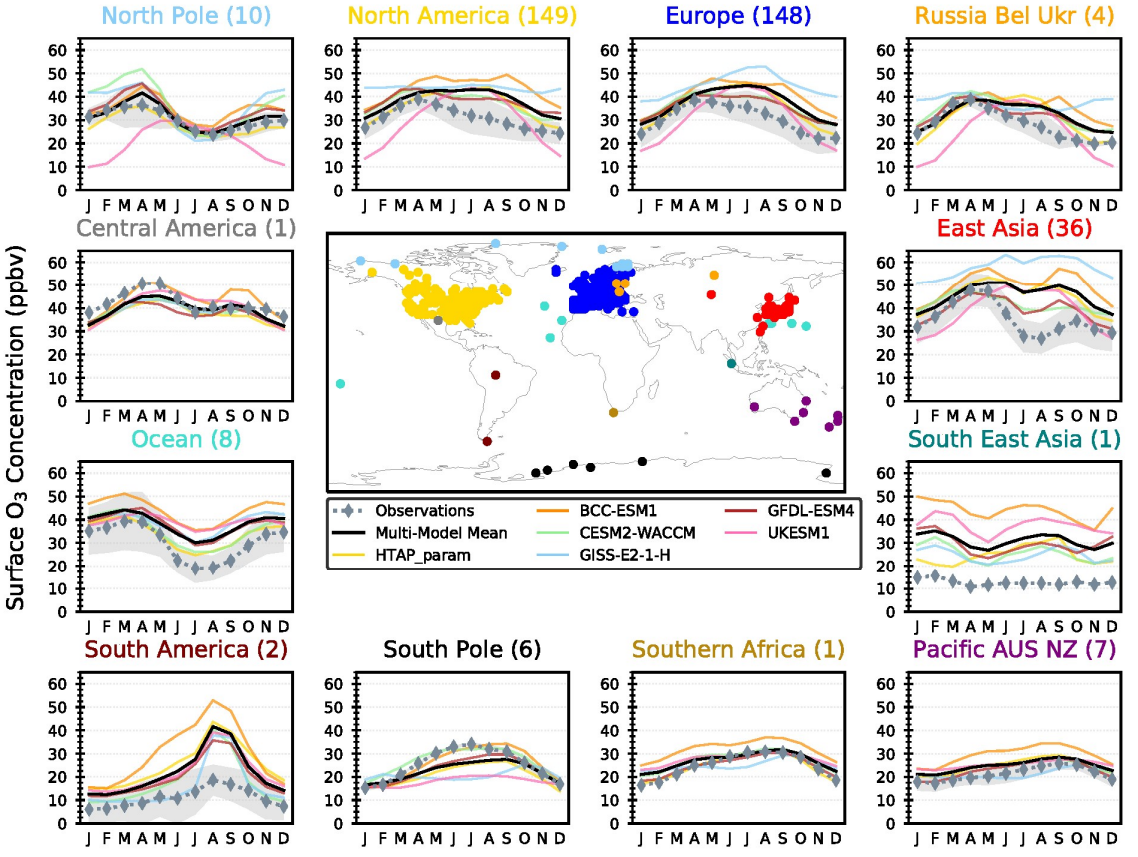

Figure 4 – Individual and multi-model (5 CMIP6 models and HTAP_param) monthly mean surface O_3 concentrations across different world regions compared with the regional monthly values from all the TOAR observations within the region for the period 2005-2014. The number of observations within a region is shown in parenthesis. The shading shows variability in observations across all sites within the region.

3.2 Surface $PM_{2.5}$

3.2.1 Ground Based Observations

A similar comparison is made for seasonal mean surface $PM_{2.5}$ concentrations from CMIP6 models against ground based surface observations (Figure 5). The seasonal multi-model mean from CMIP6 models shows that elevated $PM_{2.5}$ concentrations (>50 μg m^{-3}) occur close to the large dust emission source regions of the Sahara and Middle East in both DJF and JJA over 2000-2010. These natural source regions are also one of the largest areas of diversity in $PM_{2.5}$ concentrations (up to 20 μg m^{-3}) between the different CMIP6 models (Fig. 5b, 5e and S7). High concentrations of $PM_{2.5}$ (>40 μg m^{-3}) are also simulated over the large anthropogenic source regions of South and East Asia, particularly in DJF when there is enhanced variability

https://doi.org/10.5194/acp-2019-1211
Preprint. Discussion started: 21 January 2020

Atmospheric Chemistry and Physics Discussions

across CMIP6 models due to the different contribution from anthropogenic $PM_{2.5}$ components (Fig. S8-S10). Lower $PM_{2.5}$ concentrations (<10 μg m^{-3}) are predicted across both North America and Europe, with more agreement between CMIP6 models. Across the biomass burning regions of South America and Southern Africa, $PM_{2.5}$ are elevated in JJA with larger diversity in the CMIP6 models due to the differing contributions of the BC and OA components (Fig. S9 and S10). Relatively consistent $PM_{2.5}$ concentrations of <10 μg m^{-3}, with small model diversity (<5 μg m^{-3}), are shown across oceanic regions, mainly from emissions of sea salt (Fig. S11). Apart from the natural sources of aerosol, which are subject to meteorological variability, the CMIP6 models are relatively consistent when simulating $PM_{2.5}$ concentrations across most regions.

Compared to the ground based observations from the GASSP database, the CMIP6 multi-model mean underpredicts the observed $PM_{2.5}$ values in both seasons, with a slightly larger underestimation in DJF than JJA. As discussed in section 2.3, an underestimation was anticipated from comparing approximate $PM_{2.5}$ concentrations, derived from CMIP6 models, to observed values. Nevertheless, the evaluation highlights that fine particulate matter ($PM_{2.5}$) is generally underrepresented in the CMIP6 models across North America, Europe and parts of Asia for which observations are available; a similar result to other global and regional models (Glotfelty et al., 2017; Solazzo et al., 2017). This could be potentially due to uncertainties in emissions (e.g. local dust sources) or deposition (dry or wet), the coarse resolution of global models and absence/underrepresentation of aerosol formation processes (e.g. nitrate aerosols or secondary organic aerosols).

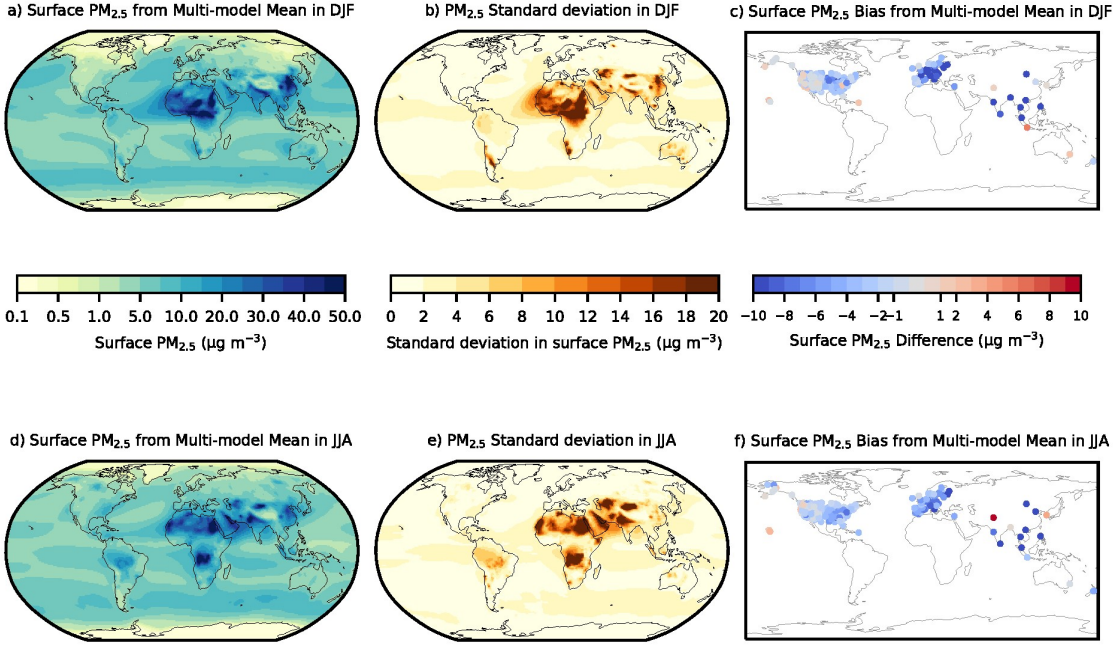

Figure 5 – Multi-model (10 CMIP6 models) seasonal mean surface $PM_{2.5}$ concentrations in a) December January, February (DJF) and d) June, July, August (JJA) over the 2000-2010 period. The standard deviation in the multi-model mean in b) DJF and e) JJA. The difference between the multi-model mean and $PM_{2.5}$ observations in c) DJF and f) JJA.

https://doi.org/10.5194/acp-2019-1211
Preprint. Discussion started: 21 January 2020

Atmospheric Chemistry and Physics Discussions

The simulated regional mean annual cycle in surface $PM_{2.5}$ from different CMIP6 models against observations is shown in Figure 6. The low model bias in $PM_{2.5}$ concentrations is highlighted across all regions, except for the ocean. Across North America, the region with most observations, the annual cycle is simulated relatively well with a peak in concentrations in JJA and a lower model bias, although a larger model bias (factor of ~1.5 to 2) occurs in winter and spring. Across Europe, there is a larger underestimation of observed $PM_{2.5}$ concentrations by CMIP6 models in DJF (factor > 2) than JJA. Nitrate aerosols are observed and modelled (Fig. S12) to contribute between 1 and 5 μg m^{-3} of the total aerosol mass over Europe (Fagerli and Aas, 2008; Pozzer et al., 2012), explaining part, but not all, of the model observational discrepancy here. Additionally, on Fig. 6 the CMIP6 models also underestimate the MERRA-2 reanalysis product (which does not include nitrate aerosols), indicating that other aerosol sources/processes are underrepresented across Europe and other regions in the models. The limited number of observations across other regions makes it difficult to infer particular model/observational biases. However, over Asia CMIP6 $PM_{2.5}$ concentrations tend to be within a factor of 2 of the observations and represent the seasonal cycle relatively well at these locations. Across South Asia, concentrations are relatively well simulated in JJA but a larger discrepancy exists in DJF between the model and observations.

https://doi.org/10.5194/acp-2019-1211
Preprint. Discussion started: 21 January 2020

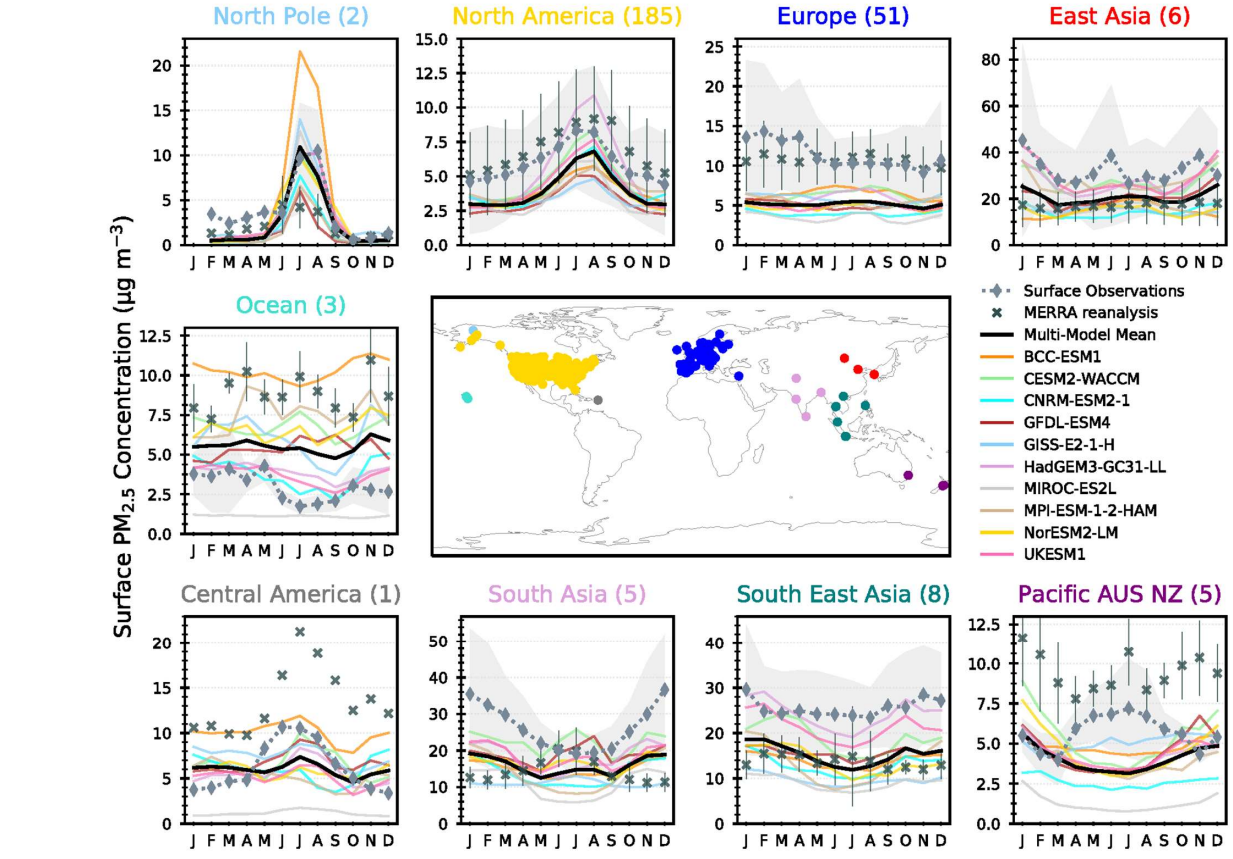

Figure 6 – Individual and multi-model (10 CMIP6 models) monthly mean surface $PM_{2.5}$ concentrations across different world regions compared with the regional monthly values from all the $PM_{2.5}$ observations (◊) and the MERRA-2 reanalysis product (x) within the region for the period 2000-2010. The number of observations within the region is shown in parenthesis. The shading and errors bars show variability in observations and the reanalysis product across all sites within the region.

3.2.2 MERRA Reanalysis Product

An additional comparison of surface $PM_{2.5}$ concentrations from the MERRA-2 aerosol reanalysis product is made with that simulated by the CMIP6 models to improve the spatial coverage and provide a more consistent evaluation of the approximate $PM_{2.5}$ concentrations. Figure 7 shows the same comparison as in Fig. 5 but now using the approximate $PM_{2.5}$ obtained from the MERRA-2 reanalysis product over the period 2005-2014. In comparison to MERRA-2, the CMIP6 models are shown to underpredict $PM_{2.5}$ concentrations across North America, Europe and Eurasia. A similar seasonal cycle comparison is shown for Europe and North America (regions with most ground based observations) in both Fig. 6 and 8, providing confidence that the underestimation of $PM_{2.5}$ by CMIP6 models is robust over these regions. Across all other regions, the MERRA-2 reanalysis

https://doi.org/10.5194/acp-2019-1211
Preprint. Discussion started: 21 January 2020

Atmospheric Chemistry and Physics Discussions

product provides much greater spatial coverage for each region and therefore the features shown in the site-level comparison (Fig. 6) will not necessarily apply here. A large overestimation of the MERRA-2 reanalysis product by the CMIP6 multi-model mean is shown across East and South Asia. Figure 8 shows that on a regional mean basis most CMIP6 models are within the spread of the MERRA-2 concentrations for East Asia, although MERRA-2 was previously shown to underestimate $PM_{2.5}$ concentrations across East Asia (Buchard et al., 2017; Provençal et al., 2017) and also on Fig. 6. CESM2-WACCM is the exception to this with distinctly higher $PM_{2.5}$ concentrations over East Asia, potentially due to larger OA concentrations and more dust aerosols within the western side of this region (Fig. S7 and S10). Across the South Asian region, CMIP6 models show a more consistent overestimation of MERRA-2, with UKESM1 and CESM2-WACCM showing particularly high $PM_{2.5}$ concentrations, again due to dust and OA. Across North Africa there is a lot of inter-regional variability with CMIP6 models both under and over-estimating the MERRA-2 $PM_{2.5}$ concentrations, although this results in a relatively good regional mean representation (Fig. 7 and 8). The annual mean cycle in MERRA-2 $PM_{2.5}$ concentrations across South America is well represented by the CMIP6 models, although the peak in the biomass burning season is underestimated in some models. A more pronounced annual cycle is exhibited by UKESM1 across Southern Africa, potentially due to the larger contributions from the OA fraction (Fig. S10) that result from enhanced biogenic emissions leading to secondary OA formation (SOA). Across oceanic locations all of the CMIP6 models underestimate the MERRA-2 $PM_{2.5}$ concentrations, although MERRA-2 was previously shown to overestimate sea-salt concentrations (Buchard et al., 2017; Provençal et al., 2017), accounting for some of this discrepancy. Overall, comparisons of CMIP6 models with the MERRA-2 reanalysis product show biases across Europe and North America that are consistent with the comparison to ground-based observations. Additionally, similar comparisons are shown in annual mean cycles across other regions, for which appropriate ground based data is lacking.

https://doi.org/10.5194/acp-2019-1211
Preprint. Discussion started: 21 January 2020

Atmospheric Chemistry and Physics Discussions

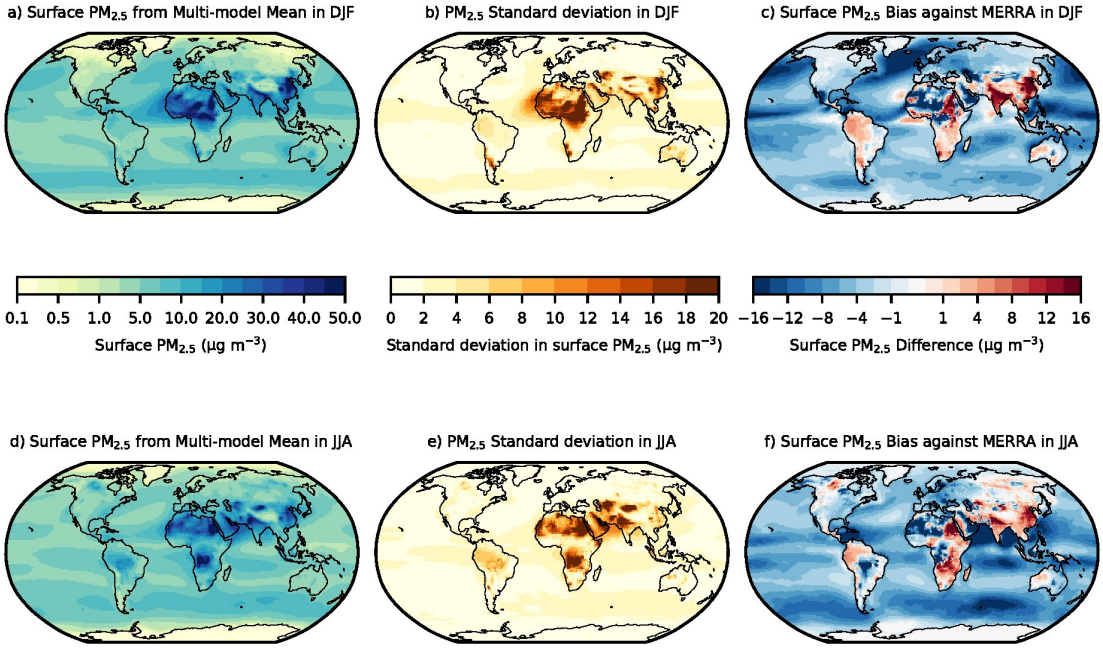

Figure 7 – Multi-model (10 CMIP6 models) seasonal mean surface $PM_{2.5}$ concentrations in a) December January, February (DJF) and d) June, July, August (JJA) over the 2005-2014 period. The standard deviation in the multi-model mean in b) DJF and e) JJA. The difference between the multi-model mean and MERRA-2 reanalysis for c) DJF and f) JJA.

https://doi.org/10.5194/acp-2019-1211
Preprint. Discussion started: 21 January 2020

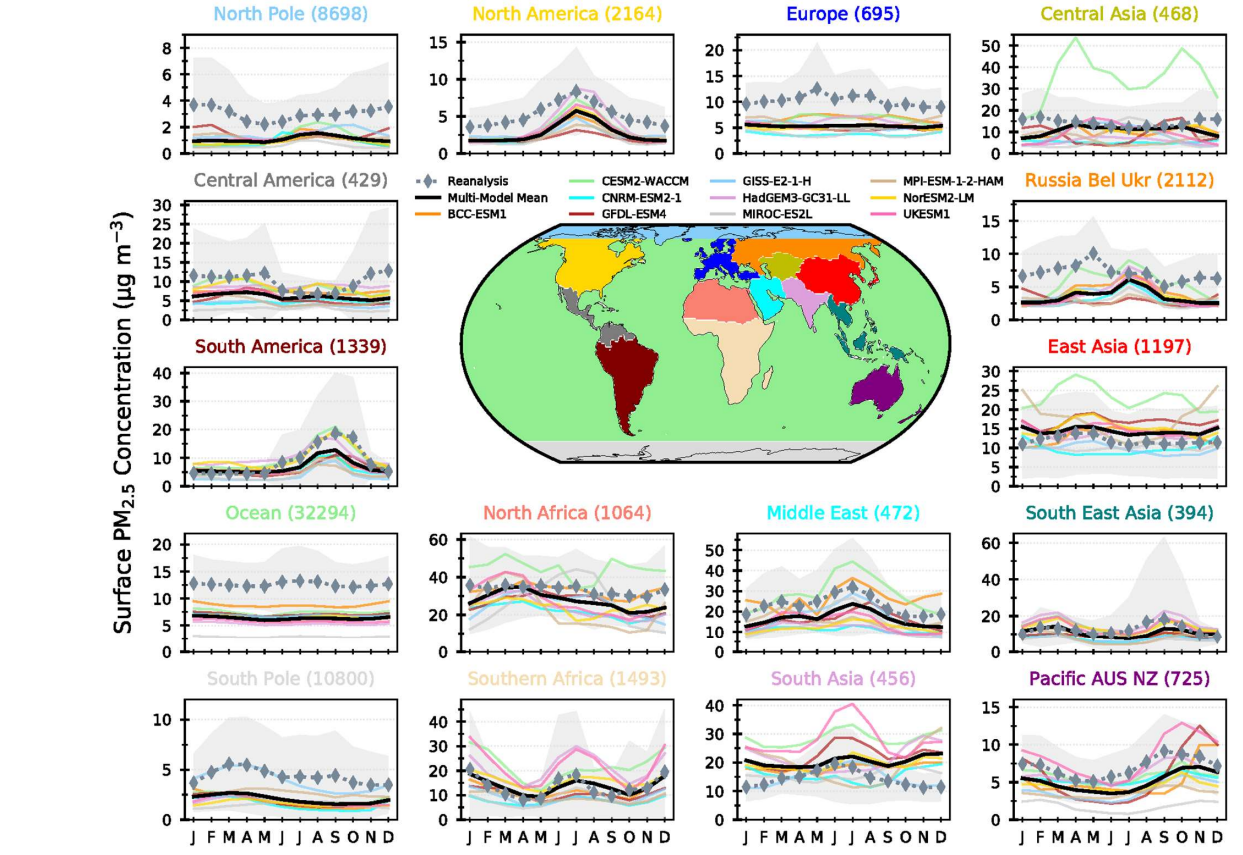

Figure 8 – Individual and multi-model (10 CMIP6 models) monthly mean surface $PM_{2.5}$ concentrations across different world regions compared with the regional monthly values from the $PM_{2.5}$ MERRA-2 reanalysis within the region for the period 2005-2014. The number of reanalysis points within the region is shown in parenthesis. The shading shows variability in the values of the MERRA-2 reanalysis products across the region.

4 Air Pollutants from Pre-Industrial to Present-day

4.1 Surface Ozone

The simulated changes in surface O_3 across 5 CMIP6 models and the HTAP_param are shown in Figure 9 over the historical period of 1850 to 2014. The CMIP6 multi-model mean shows that global annual mean surface O_3 has increased by 11.5 +/- 2.2 ppb since 1850 (+/- 1 standard deviation), although the change could be as large as 14 ppb (from BCC-ESM1) or as little as 7 ppb (from UKESM1). The 1850 to 2000 multi-model mean change in surface O_3 from the CMIP6 models of 10.6 ppb is in good agreement with the 10 +/- 1.6 ppb simulated by the CMIP5 models used in ACCMIP (Young et al., 2013). An

https://doi.org/10.5194/acp-2019-1211
Preprint. Discussion started: 21 January 2020

Atmospheric Chemistry and Physics Discussions

evaluation of the long-term changes in surface O_3 over the historical period simulated by the CMIP6 models at specific measurement locations is presented separately in Griffiths et al., (2019), which shows that the CMIP6 models are able to represent long term changes in surface ozone since the 1960s.

A large diversity in the simulated historical changes is shown across the different regions analysed here, with UKESM1 tending to simulate the lowest historical change and GISS-E2-1-H or BCC-ESM1 the highest. Even, though the surface response is small in UKESM1, it is shown to have larger tropospheric changes in O_3 over the historical compared to other CMIP6 models (Griffiths et al., 2019). South Asia is the region with the largest diversity in simulated historical changes in surface O_3 of between 16 and 40 ppb. Surface O_3 is simulated to have increased by between 10 to 30 ppb over the major northern anthropogenic source regions since 1850, driven mainly by the large increases in anthropogenic precursor emissions of CH_4, NOx, CO, and NMVOCs over this period. A qualitative estimate of the influence of non-emission driven processes (chemistry and climate change) can be ascertained by comparing results from the HTAP_param, an emission-only driven model, to those of the CMIP6-models. Simulated historical changes in surface O_3 from UKESM1 are similar to those from the HTAP_param, indicating that changes simulated by UKESM1 are strongly determined by precursor emissions. However, the global annual mean surface O_3 response of 7.6 +/- 0.7 ppb from HTAP_param over the historical period is 3.9 ppb lower than the CMIP6 multi-model mean, indicating globally that non-emission driven processes have contributed to approximately 30% of the change in surface O_3, although this contribution varies regionally. The different magnitude of response across models could be due to non-emission driven process, e.g. from different chemistry schemes and climate change signals within models.

https://doi.org/10.5194/acp-2019-1211
Preprint. Discussion started: 21 January 2020

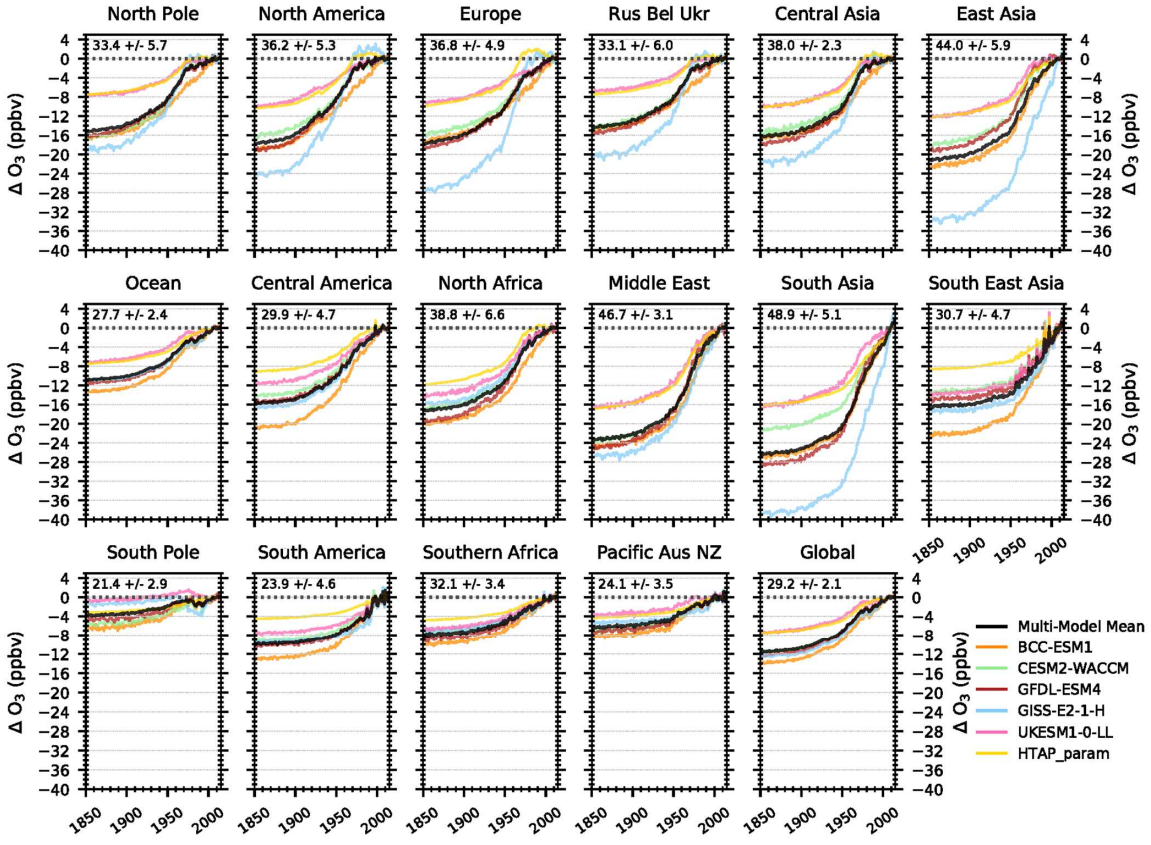

Figure 9 – Changes in the regional and global annual mean surface O_3 concentrations, relative to a 2005-2014 mean value, across 5 CMIP6 models and the HTAP_param. The multi-model annual mean year 2005-2014 surface O_3 concentrations (+/- 1 standard deviation) are shown in the top left of each panel. Regions are defined in Figure S1.

4.2 Surface $PM_{2.5}$

The simulated change in annual mean surface $PM_{2.5}$ across 10 CMIP6 models is shown in Figure 10 across the historical period of 1850 to 2014. Since 1850, CMIP6 models simulated an increase in global annual mean surface $PM_{2.5}$ concentrations of <2 μg m^{-3} (15-20%). Larger increases of surface annual mean $PM_{2.5}$ of up to 12 μg m^{-3} are simulated across South and East Asia. The historical increase in surface $PM_{2.5}$ is primarily driven by the large increase in anthropogenic aerosol and aerosol precursor emissions over the 1850-2014 period (Hoesly et al., 2018). The largest model diversity is also exhibited over the Asian regions with variations in the response between models of up to 50%, potentially due to differences in dust emissions and simulation of organic aerosols. The largest interannual variability in surface $PM_{2.5}$ concentrations occurs over the North African and Middle East regions as they are located near large sources of dust, whose emissions are highly dependent on meteorological

https://doi.org/10.5194/acp-2019-1211
Preprint. Discussion started: 21 January 2020

Atmospheric Chemistry and Physics Discussions

fluctuations (wind speed). Over Europe, and to a lesser extent Russia, Belarus, Ukraine and North America, the increase in surface $PM_{2.5}$ concentrations since 1850 peaked in the 1980s at 4 µg m^{-3} above the 2005-2014 mean value before decreasing over the last 30 years. This change is consistent with both observations and simulated changes in aerosols over this period in response to emission reductions from the implementation of air quality legislation (Leibensperger et al., 2012; Tørseth et al., 2012; Daskalakis et al., 2016; Turnock et al., 2016; Archibald et al., 2017).

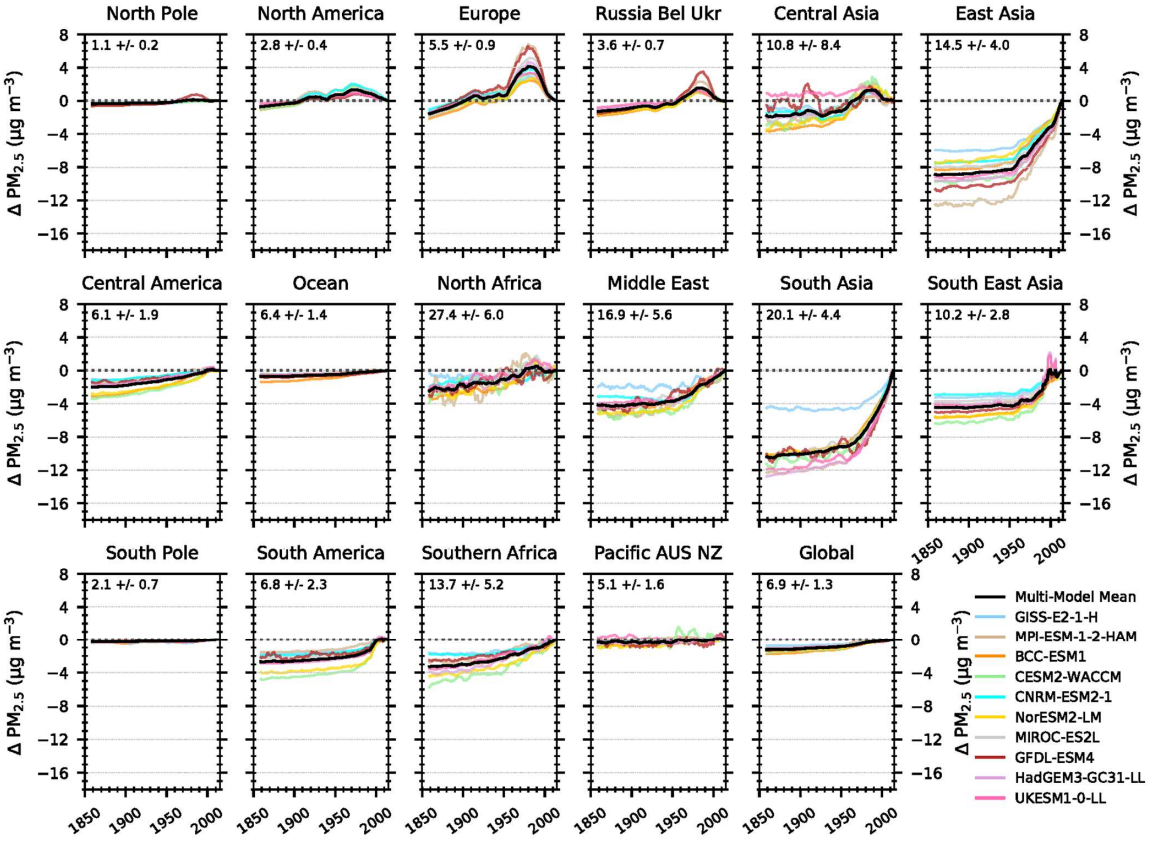

Figure 10 – Changes in the regional and global annual mean surface $PM_{2.5}$ concentrations, relative to a 2005-2014 mean value, across 10 CMIP6 models. Changes for each region are computed as 10 year running means over the historical period. The multi-model mean 2005-2014 surface $PM_{2.5}$ concentrations (+/- 1 standard deviation) are shown in the top left of each panel. Regions are defined in Figure S1.

https://doi.org/10.5194/acp-2019-1211
Preprint. Discussion started: 21 January 2020


Atmospheric Chemistry and Physics Discussions

5 Air Pollutants from Present-day to 2100

An analysis is now made of the future projections of air pollutants in the CMIP6 Tier 1 scenarios, including ssp370-lowNTCF. A comparison is made of the projected future changes by 2050 and 2100 in four CMIP6 models which had the most data available for the ssp370 scenario.

5.1 Surface Ozone

Global annual mean surface O_3 is reduced by more than 4 +/- 0.5 ppb (+/- 1 standard deviation value of the multi-model mean) in the near-term (2050) and by 8 +/- 1.0 ppb in 2100 in the strong air pollutant and climate mitigation scenario ssp126 (Figure 11). Smaller reductions in global annual mean surface O_3 are predicted for the middle of the road pathway (ssp245) of 3 +/- 0.1 ppb by 2100. Whereas for the weak climate and air pollutant mitigation scenario ssp370, a global annual mean increase in surface O_3 of 1.8 +/- 0.8 ppb in 2050 and 1.0 +/- 0.9 ppb is predicted by 2100. However, implementing strong emission controls for NTCFs on top of a weak climate mitigation scenario (ssp370-lowNTCF) shows that previous increases in global annual mean surface O_3 can be substantially reduced to values that are 2 +/- 0.4 ppb below the 2005-2014 mean value in 2050, with benefits to air quality and climate (Allen et al., 2019). For ssp585, which has weak climate mitigation measures but strong air pollution controls, a near-term increase in global annual mean surface O_3 of 2 +/- 0.7 ppb is predicted in 2050 but by 2100 surface O_3 reduces by 4 +/- 0.8 ppb, relative to 2005-2014, due to the implementation of air pollutant controls in the latter half of the 21st Century.

The global response in annual mean surface O_3 concentrations to the different scenarios is also repeated across the different world regions, albeit with differing magnitudes. In ssp370 increases in annual mean surface O_3 are predicted to occur across North America (+1.9 ppb), Europe (+4.8 ppb) and East Asia (+7.5 ppb), with the largest increase predicted in South Asia of 9.7 +/- 3.7 ppb by 2100. Surface O_3 increases across most world regions in this scenario can be attributed to the large increase in global CH_4 abundances (80%) and the large predicted increase in surface temperatures (Figure S13), despite the reductions in O_3 precursor emissions across North America, Europe and East Asia (Fig. 2). South Asia shows the largest increase in surface O_3 as precursor emissions are anticipated to increase across this region on top of the large climate change signal and growth in CH_4 abundance. Additionally, the largest diversity in predictions between the CMIP6 models is shown over South Asia, indicating that there is some disagreement between the models as to the magnitude and extent of changes over this region. Surface O_3 across oceanic regions (background) are predicted to remain at or near current values in ssp370 due to the increases in water vapour in a warming world leading to more O_3 destruction (Doherty et al., 2013). The impact of more aggressive near-term reductions to emissions of NTCFs (but not CH_4) on top of the ssp370 pathway is shown by the changes in the ssp370-lowNTCF. In this pathway surface O_3 concentrations are reduced globally and across most regions to be at or near 2005-2014 values, a substantial benefit to surface O_3 air quality compared to ssp370. Surface O_3 concentrations are predicted to have almost halved by 2050 across South Asia in ssp370-lowNTCF. However, across East Asia the additional precursor emission

https://doi.org/10.5194/acp-2019-1211
Preprint. Discussion started: 21 January 2020

Atmospheric Chemistry and Physics Discussions

reductions in ssp370-lowNTCF have made little difference to surface O_3 concentrations predicted by the CMIP6 models, indicating that other factors are more important over this region (chemistry or climate change).

Surface O_3 concentrations predicted across northern hemisphere regions in ssp585 are similar to ssp370 due to comparable changes in air pollutant emissions and climate change. However, a notable exception is a reduction in surface O_3 across regions towards the latter half of the 21st Century (post 2080) when there are additional reductions in precursor emissions and global CH_4 abundances by 2100. Surface O_3 is predicted to stay at or near 2005-2014 values until 2040 over South Asia in ssp585. This is despite increases in precursor emissions and changes in climate, indicating that there are potentially some changes in chemical O_3 formation across this region in this scenario that constrain any increases in surface O_3.

The future scenario ssp245 (middle-of-the-road) predicts annual mean surface O_3 concentrations that tend to remain at or near the 2005-2014 mean values by 2100 across the major anthropogenic source regions of the Northern Hemisphere, whereas for other tropical and southern hemisphere regions surface O_3 concentrations are reduced by up to 4 ppb. The changes in ssp245 are driven by larger precursor emission controls, a smaller climate change signal and controlling CH_4 so that global abundances are just below 2015 values by 2100 (Fig. 1g). In ssp245 a near-term (up to 2040) increase in surface O_3 is shown across Europe, East Asia and South Asia, which could be attributed to the peaking of global CH_4 abundances at this point prior to then reducing.

The Tier1 future scenario with the strongest climate and air pollutant mitigation measures, ssp126, shows substantial decreases in surface O_3 concentrations across most regions due to the large reduction in precursor emissions, global CH_4 abundances, and small climate change signal. Reductions in surface O_3 of more than 8 ppb are predicted across anthropogenic emission source regions of the northern hemisphere, with smaller reductions across southern hemisphere regions.

Predictions from the CMIP6 models show that to achieve global benefits for regional surface O_3 it is important to control O_3 precursor emissions (including CH_4) in addition to limiting future climate change. However, scenarios with large increases in global CH_4 abundances, a large climate change signal and limited control of precursor emissions fail to restrict regional increases in surface O_3, leading to poor future air quality and potential human health impacts (Silva et al., 2017).

https://doi.org/10.5194/acp-2019-1211
Preprint. Discussion started: 21 January 2020

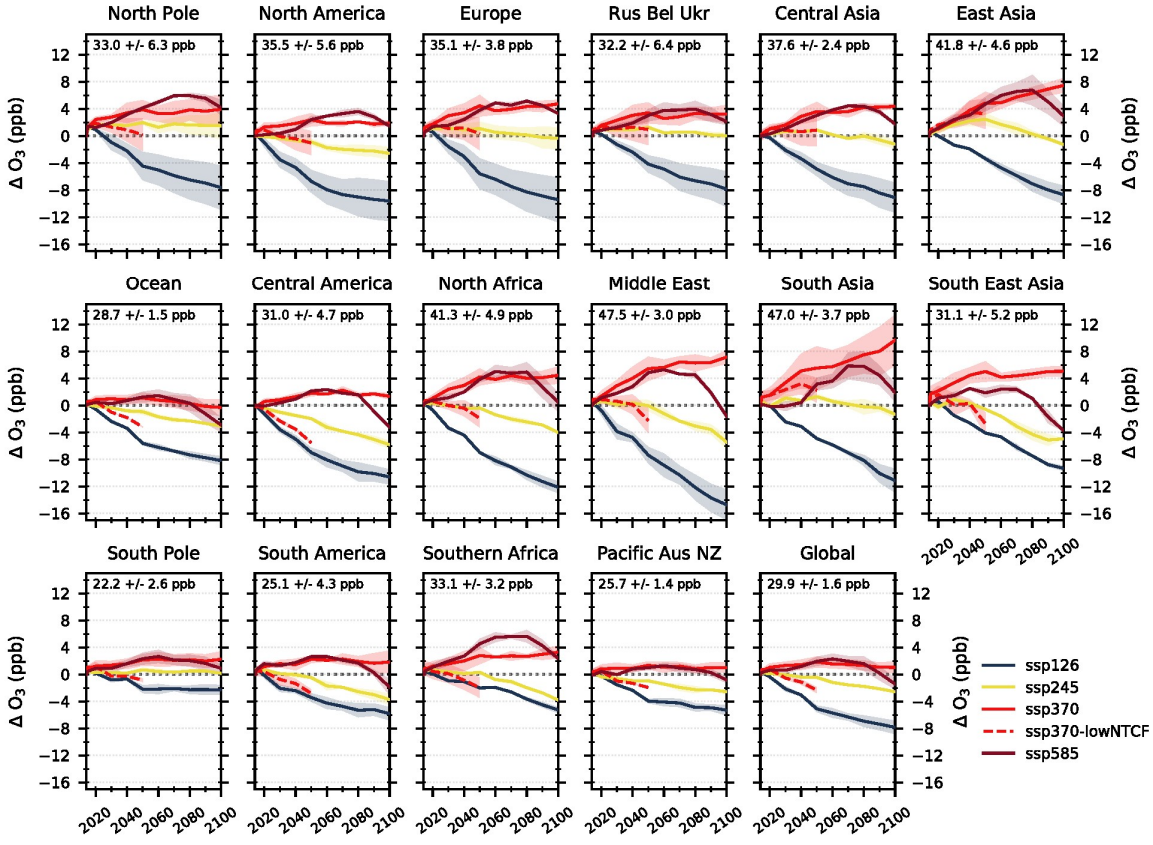

Figure 11 – Future global and regional changes in annual mean surface O_3, relative to 2005-2014 mean, for the different SSPs used in CMIP6. Each line represents a multi-model mean across the region with shading representing the +/- 1 standard deviation in the mean. See Table 1 for details of models contributing to each scenario. The multi-model regional mean value (+/- 1 standard deviation) for the year 2005-2014 is shown in the top left corner of each panel.

A more detailed comparison of future surface O_3 predictions between CMIP6 models has been undertaken for ssp370, as it is the scenario with the largest number of available models (Table 1). The regional change in decadal mean surface O_3, relative to 2005-2014, in 2050 (2045 - 2055 mean) and 2095 (2090 – 2100 mean) for ssp370 from four CMIP6 models and the HTAP_param is shown in Figure 12. Discrepancies in the simulated response of background O_3 across the ocean region (also South Pole and Pacific, Australia and New Zealand) are noticeable between individual models, with UKESM1 predicting a decrease in surface O_3 compared to the small increase from the HTAP_param and other models in both 2050 and 2095 (Figure S14). UKESM1 is a model with high equilibrium climate sensitivity (ECS, 5.4 K) compared to other CMIP6 models (Forster et al., 2019; Sellar et al., 2019), and therefore will exhibit a larger climate response (surface temperature and water vapour) leading to enhanced background O_3 destruction via water vapour and the hydroxyl radical (OH). Over the North Pole region

https://doi.org/10.5194/acp-2019-1211
Preprint. Discussion started: 21 January 2020


Atmospheric Chemistry and Physics Discussions

all models show surface O_3 increases that are larger than the HTAP_param, indicating that the large temperature response or changes to long-range transport could be an important driver over this region with comparatively low local emissions.

Differences in the predicted surface O_3 between models exist across South Asia where CESM2-WACCM (and BCC-ESM1 in 2050) predict a response that is twice as large as UKESM1 and GFDL-ESM4. The large increase in NOx emissions in this scenario over South Asia (~80%) has resulted in areas of NOx titration near the Indo-Gangetic plain in both UKESM1 and GFDL-ESM4, reducing surface O_3 concentrations (Fig. S14). This feature of NOx titration of O_3 is absent in both CESM2-WACCM and BCC-ESM1, resulting in larger O_3 production over South Asia. The comparison in Fig. 12 shows how the O_3 chemistry within models responds differently in a future scenario with a large climate change signal and over a region with large increases in local precursor emissions.

Over South America and Southern Africa, particularly the tropical areas (Fig. S14), larger future changes in surface O_3 are predicted by GFDL-ESM4/UKESM1 than CESM2-WACCM. Over this region, biogenic emissions (particularly isoprene) are an important source of O_3 formation. Discrepancies in the magnitude of change in these emissions due to climate and land-use change could lead to the inter-model differences in surface O_3. Total emissions of BVOCs (isoprene and monoterpenes) and their future change in ssp370 obtained from three models (Figure S15) show that CESM2-WACCM has larger emissions over the period 2005-2014 which increase in the future ssp370 scenario. Whereas, GFDL-ESM4 and UKESM1 have smaller increases in BVOC emissions with some emissions reducing over parts of Africa in UKESM1. The BVOC emission changes appear to have affected the future O_3 formation differently in the individual models over these regions and represents an important process to understand further.

Whilst there is disagreements between models over some regions, there is substantial consistency in the predicted increase to surface O_3 in ssp370 over North America, Europe and East Asia, which is larger than that from HTAP_param. However, BCC-ESM1 tends to predict a larger increase than the other three models, potentially due to the coarser resolution of this ESM. As most anthropogenic precursor emissions are decreasing in this scenario across all these regions, changes in climate and global CH_4 abundances seem to be the major driver of surface O_3 increases.

The differences between the individual CMIP6 models highlight the importance of further understanding how future O_3 chemistry is affected by changes to precursor emissions and climate. The predicted differences in models can be quite pronounced over regions like South Asia where changes in one model can be double that of another model, which could have important consequences for future regional air quality.

https://doi.org/10.5194/acp-2019-1211
Preprint. Discussion started: 21 January 2020

Atmospheric Chemistry and Physics Discussions

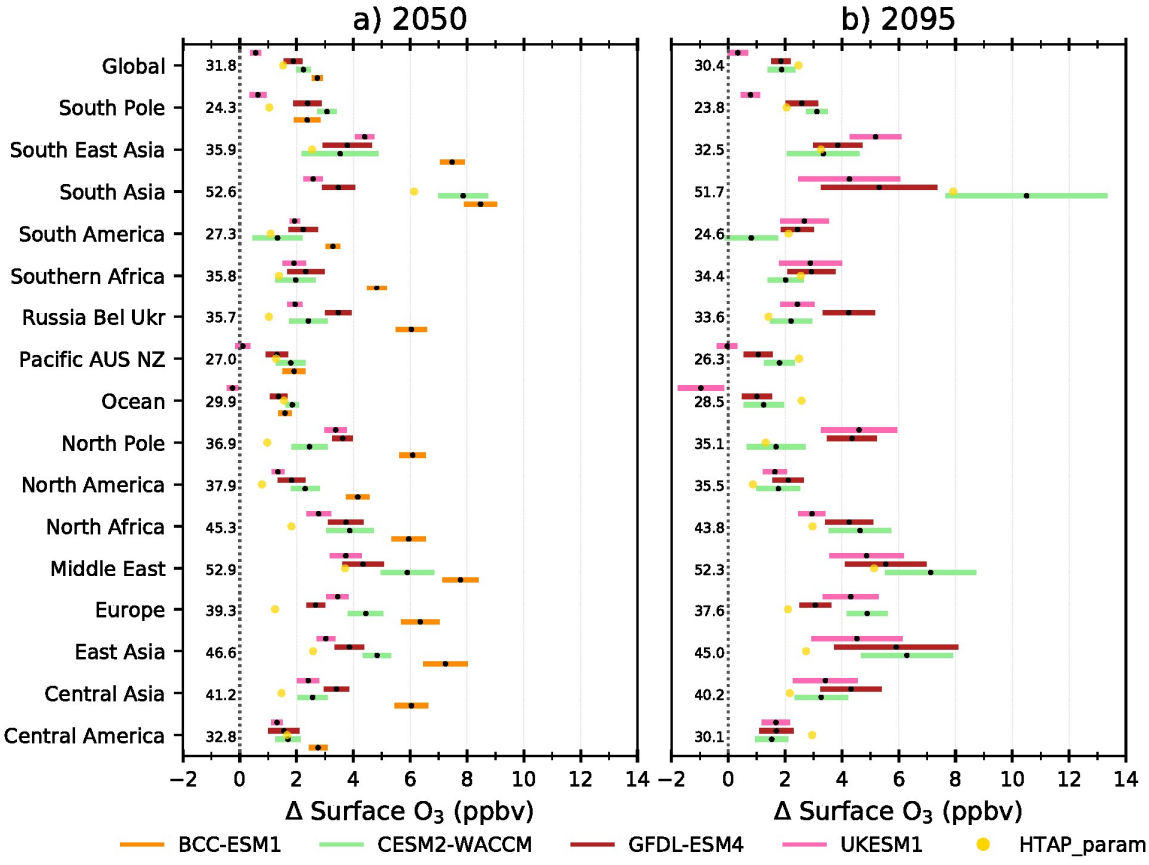

Figure 12 – Future global and regional changes in the decadal annual mean surface O_3, relative to the 2005-2014 mean, for the ssp370 pathway used in CMIP6. Each black circle represents the decadal mean response for an individual model in a) 2045-2055 and b) 2090-2100, with the coloured bars showing the standard deviation across the decadal mean. The multi-model regional mean over the period 2005- 2014 is given towards the left of each panel. The response from the HTAP_param in each time period is shown by the separate gold circle.

5.2 Surface $PM_{2.5}$

Relatively small global changes in annual mean surface $PM_{2.5}$ are predicted for all CMIP6 models across all scenarios, with an increase in ssp370 and a reduction in the others. Small reductions in $PM_{2.5}$ are predicted for all scenarios across Europe (0.3 to 3 μg m^{-3}) and North America (0.1 to 1.3 μg m^{-3}) due to the reduction in aerosol and aerosol precursor emissions. Differences in $PM_{2.5}$ between scenarios are highlighted across a number of regions.

For the weak climate and air pollutant mitigation scenario ssp370, increases in annual mean surface $PM_{2.5}$ are predicted across South Asia (7.4 +/- 3.4 μg m^{-3} by 2050 and 4.3 +/- 3.0 μg m^{-3} by 2100), South East Asia (3.0 +/- 5.3 μg m^{-3} by 2100), Southern Africa (1.9 +/- 4.5 μg m^{-3} by 2100), Central (3.3 +/- 3.5 μg m^{-3} by 2100) and South America (3.1 +/- 3.6 μg m^{-3} by 2100). The

https://doi.org/10.5194/acp-2019-1211
Preprint. Discussion started: 21 January 2020


Atmospheric Chemistry and Physics Discussions

increases in $PM_{2.5}$ are driven mainly by the increase in aerosol and aerosol precursor emissions in this scenario (Fig. 2). However, there is a degree of uncertainty associated with all of these future predictions indicated by the large diversity across the CMIP6 models. Some of the largest predicted increases in surface $PM_{2.5}$ occur across South Asia in ssp370, a region already with high present day $PM_{2.5}$ concentrations. The increase in $PM_{2.5}$ peak in 2050 across this region, which coincides with the increase of SO_2, BC and OC emissions, before declining to 2100 when emissions reduce. Over East Asia, annual mean $PM_{2.5}$ concentrations are simulated to remain at or near 2005-2014 values until the latter half of the 21st Century when the decrease in emissions reduce $PM_{2.5}$ concentrations by 2.8 +/- 2.6 µg m^{-3}. The impact of reductions in NTCFs on top of the ssp370 scenario act to constrain any increases of $PM_{2.5}$ concentrations to near present day values across most regions. However, substantial reductions in $PM_{2.5}$ concentrations of 5.6 +/- 2.1 µg m^{-3} and 5.9 +/- 1.4 µg m^{-3} below 2005-2014 values are achieved across East and South Asia respectively, by implementing these measures. Due to the short lifetime of aerosols in the atmosphere $PM_{2.5}$ concentrations respond rapidly to the large cuts in emissions that occur in ssp370-lowNTCF and show the benefits to targeting these emissions, although there could be a potential climate impact (Allen et al., 2019).

Reductions in annual mean surface $PM_{2.5}$ are simulated across all regions for ssp126, ssp245 and ssp585. Differences exist in the magnitude and timing of $PM_{2.5}$ reductions across regions linked to the changes in emissions. The largest reductions in $PM_{2.5}$ occur over South Asia in 2100 and range from 12.1 +/- 1.9 µg m^{-3} in ssp126 to 9.1 +/- 1.9 µg m^{-3} in ssp585, a substantial benefit to regional air quality. Similar benefits to $PM_{2.5}$ are achieved over East Asia by 2100 although the more rapid improvements occur over this region in the first part of the 21st Century.

The response of $PM_{2.5}$ concentrations is more variable, with a larger diversity across CMIP6 models within regions that are close to natural aerosol emission sources. This is particularly noticeable over North Africa where the variability across CMIP6 models in dust emissions from the Saharan source region (Fig. S7) results in an uncertain $PM_{2.5}$ response across this region. A similar response is also exhibited across the Middle East and Central Asia. The potential influence of BVOCs on SOA formation (Fig. S15 and S18) could also be contributing to the diversity in the CMIP6 model responses across the South America and Southern Africa regions.

The CMIP6 models show that future reductions in aerosols and aerosol precursors will lead to a decrease in surface $PM_{2.5}$ concentrations across most world regions and a benefit to regional air quality (and human health), consistent with that from CMIP5. However if emissions are not controlled over economically developing regions such as South America, Asia and Africa then surface $PM_{2.5}$ is anticipated to increase and worsen future regional air quality. Targeting emission reductions of NTCFs in the short-term shows the potential for rapid improvements in surface $PM_{2.5}$ and air quality.

https://doi.org/10.5194/acp-2019-1211
Preprint. Discussion started: 21 January 2020

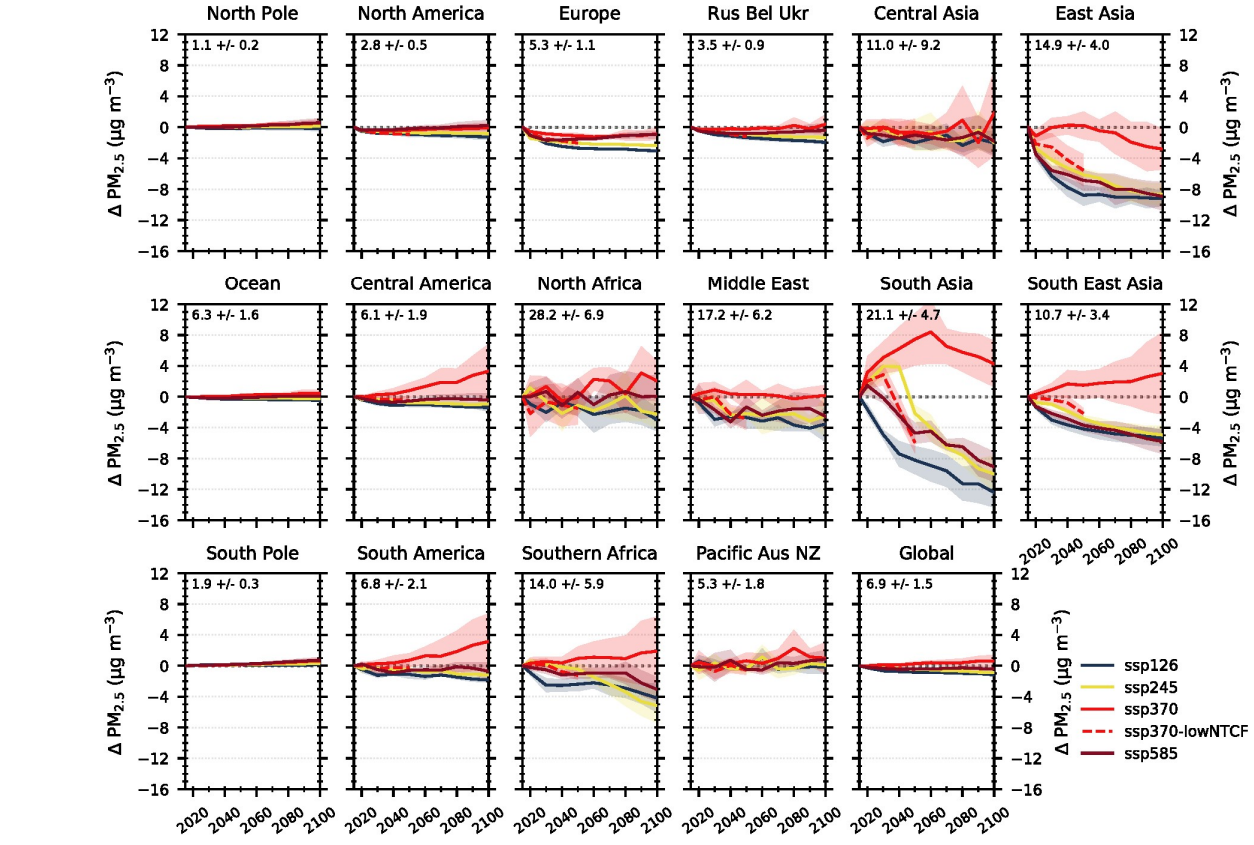

Figure 13 – Future global and regional changes in annual mean surface $PM_{2.5}$, relative to 2005-2014 mean, for the different SSPs used in CMIP6. Each line represents a multi-model mean across the region with shading representing the +/- 1 standard deviation in the mean. See Table 1 for details of models contributing to each scenario. The multi-model regional mean value (+/- 1 standard deviation) for the year 2005-2014 is shown in the top left corner of each panel.

In a similar analysis to surface O_3, a more detailed comparison has been undertaken of four CMIP6 models predicting changes in surface $PM_{2.5}$ in 2050 and 2095 under ssp370 (Figure 14). Small reductions in surface $PM_{2.5}$ concentrations (<2 µg m^{-3}) are simulated consistently by all CMIP6 models across North America and Europe in ssp370, mainly attributed to decreases in the BC and SO_4 components. South Asia, the region with the largest simulated future change in surface $PM_{2.5}$ of up to 12 µg m^{-3}, shows fairly good agreement between three CMIP6 models (UKESM1, GFDL-ESM4 and CESM2-WACCM) as predictions in 2050 and 2095 are all within the range of each of the individual models. The MIROC-ES2L model predicts smaller future increases in surface $PM_{2.5}$ than the other models across South Asia of up to 5 µg m^{-3} in both 2050 and 2095. This is a result of smaller changes in the BC, OA and sulphate aerosol components in the MIROC-ES2L model despite increases in aerosols and aerosol precursor emissions across South Asia in ssp370 (Figure S16-S18).

https://doi.org/10.5194/acp-2019-1211
Preprint. Discussion started: 21 January 2020


Atmospheric Chemistry and Physics Discussions

Disagreements in both the sign and magnitude of simulated future surface $PM_{2.5}$ changes between CMIP6 models are also exhibited across East Asia. Small regional mean increases are predicted in 2050 for all models apart from GFDL-ESM4, attributed to a larger reduction in SO_4 than other models across this region (Fig S17). In 2095 most models, apart from CESM2-WACCM, simulate a reduction in $PM_{2.5}$ concentrations across East Asia. All models simulate continual reductions out to 2100 for SO_4 across this region, whereas BC increases in the near-term before decreasing out to 2100. For OA, CESM2-WACCM shows larger increases over East Asia in both 2050 and 2095 compared to the other models, which show a smaller increase in 2050 and a reduction by 2095 (Fig. S18). CESM2-WACCM includes a more complex treatment of SOA formation, showing a strong response to climate and historical trends in OA (Tilmes et al., 2019), which could explain the multi-model differences across East Asia. The discrepancies in CMIP6 models are not as obvious over South Asia as the effect of the increase in OA over South Asia in CESM2-WACCM is masked by coincident increases in other components across other models. CESM2-WACCM also shows larger simulated increases in $PM_{2.5}$ over South America, Central America, Southern Africa and South East Asia than other models, which can be attributed to the larger increase in the OA fraction in this model. However, over Southern Africa UKESM1 shows a reduction in future $PM_{2.5}$, in contrast to the other models. This can again be attributed to a reduction in the OA fraction in UKESM1 (Fig. S18), related to potential changes in land use and a reduction in biogenic emissions (monoterpenes) across Southern Africa in ssp370 (Fig. S15), the main precursor to SOA formation in this model (Mulcahy et al., 2019).

The decadal mean $PM_{2.5}$ response is variable across individual CMIP6 models over regions close to natural sources of particulate matter (North Africa, Central Asia and Pacific, Australia and New Zealand). Over these regions there is a large range in both the sign and magnitude of the $PM_{2.5}$ response, which can be mainly attributed to the dust fraction (Fig. S19) and the fact that this aerosol source has a large inter-annual variability in its emission strength. Interestingly, the CMIP6 models do not agree in the sign and magnitude of future changes to dust concentrations in ssp370 (Fig. S19).

Across the ocean and North Pole regions all the CMIP6 models tend to simulate a small increase in $PM_{2.5}$ concentrations, which can be attributed to increases in sea salt concentrations (Fig. S20). A strong increase in all models is simulated across the Southern Ocean (and other oceans), potentially driven by changes to meteorological conditions which increase wind speed and sea salt emissions. As ssp370 is a scenario with a large climate change signal, the increases in $PM_{2.5}$ across the North Pole can be attributed to the melting of sea ice increasing sea salt emissions. However, the magnitude of this response is different in the CMIP6 models due to the underlying ECS and the response of Arctic surface temperatures within the individual model. The differences in the simulated future $PM_{2.5}$ changes across the CMIP6 models in ssp370 highlight that it is important to consider how natural sources of aerosol respond in a future climate in addition to that from changes in anthropogenic emissions. Particular differences between models have been shown for dust, sea salt and also organic (secondary) aerosols, which should be explored further. In addition, the different representations of aerosols within individual models e.g. organic aerosols, are an important consideration as they can make a large difference to any future regional prediction of $PM_{2.5}$.

https://doi.org/10.5194/acp-2019-1211
Preprint. Discussion started: 21 January 2020

Atmospheric Chemistry and Physics Discussions

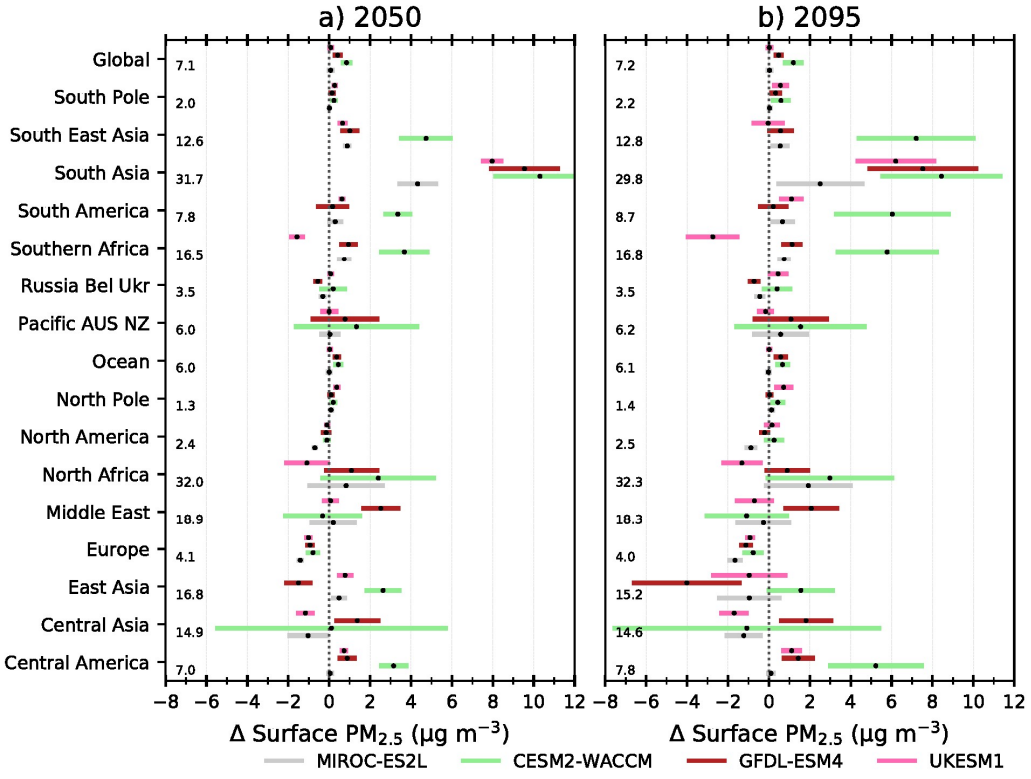

Figure 14 – Future global and regional changes in the decadal annual mean surface $PM_{2.5}$, relative to the 2005-2014 mean, for the ssp370 pathway used in CMIP6. Each black circle represents the decadal mean response for an individual model in a) 2045-2055 and b) 2090-2100, with the coloured bars showing the standard deviation across the decadal mean. The multi-model regional mean over the period 2005- 2014 is given towards the left of each panel.

6 Conclusions

In this study we have provided an initial analysis of the historical and future changes in air pollutants (O_3 and $PM_{2.5}$) from the latest generation of Earth system and climate models that have submitted results from experiments conducted as part of CMIP6. Data was available from the historical experiments of 5 CMIP6 models for surface O_3 and 10 models for surface $PM_{2.5}$. Historical changes in regional concentrations of O_3 and $PM_{2.5}$ are presented over the period 1850 to 2014 using data from all models. A present day model evaluation of the CMIP6 models was conducted against surface observations of O_3 and $PM_{2.5}$ obtained from the TOAR and GASSP databases respectively. An additional comparison was performed for simulated $PM_{2.5}$ concentrations against the MERRA-2 aerosol reanalysis product. An assessment is then made of the changes in surface O_3 and $PM_{2.5}$ simulated by the CMIP6 models across different future scenarios, ranging from weak to strong air pollutant and climate mitigation.

https://doi.org/10.5194/acp-2019-1211
Preprint. Discussion started: 21 January 2020


Atmospheric Chemistry and Physics Discussions

The 5 CMIP6 models simulate present day (2005-2014) surface O_3 concentrations that are elevated in the Northern Hemisphere summer, with lower values throughout the year across the Southern Hemisphere. However, a large model diversity is shown across the continental Northern Hemisphere due to the large simulated seasonal cycles in certain models. Compared to surface O_3 measurements, CMIP6 models consistently overpredict observed values in both summer and winter across most regions. An exception to this is at observation locations across Antarctica where CMIP6 models tend to underpredict observed values. Large surface $PM_{2.5}$ concentrations are simulated in CMIP6 models near dust and anthropogenic emission source regions. Model diversity across the CMIP6 models is largest near the dust source regions due to their sensitivity to meteorological variability, whereas across other regions the CMIP6 models are relatively similar in their simulation of $PM_{2.5}$ concentrations. Evaluating the approximate $PM_{2.5}$ calculated from CMIP6 models (excluding nitrate aerosols) against ground based $PM_{2.5}$ observations shows a consistent underprediction across most regions. The underestimation of observations by models is larger in the northern hemisphere winter than summer, in part due to the absence of nitrate aerosols within most CMIP6 models and also due to underrepresentation of other aerosol processes within the global models. To improve the spatial coverage and consistency of the $PM_{2.5}$ evaluation with CMIP6 models an additional comparison was made to the MERRA-2 aerosol reanalysis product. A similar underestimation of $PM_{2.5}$ concentrations over Europe and North America was found in the comparison of CMIP6 models and MERRA-2, providing confidence in this result from the ground-based comparison. CMIP6 models overestimated the $PM_{2.5}$ concentrations in MERRA-2 over South and East Asia, contrary to the evaluation using ground based observations. Annual mean cycles simulated by CMIP6 models and MERRA-2 tend to agree across other regions for which there are no suitable ground-based observations.

Across the historical period (1850-2014), the CMIP6 models simulated a global annual increase in surface O_3 of between 7 and 14 ppb. A global multi-model mean increase of 11.5 +/- 2.2 ppb was simulated by the CMIP6 models which agrees well with the change previously simulated by CMIP5 models. A large diversity in the historical change of surface O_3 was simulated by CMIP6 models across South Asia and other Northern Hemisphere regions. CMIP6 models predicted larger historical changes in surface O_3 than those from an emission-only driven parameterisation, indicating a potential climate change impact (Bloomer et al., 2009; Rasmussen et al., 2013; Colette et al., 2015) on surface O_3 over the historical period. Small global increases in surface $PM_{2.5}$ are simulated over the historical period by CMIP6 models, with larger regional changes of up to 12 $\mu g\ m^{-3}$ across East and South Asia. The largest diversity in the response of CMIP6 models occurs over Asian regions, with large interannual variabilities near dust source regions. CMIP6 models simulate the peak in $PM_{2.5}$ concentrations in the 1980s across Europe and North America, prior to the decline in concentrations to present day resulting from air pollutant emission controls over these regions.

The CMIP6 models predict surface O_3 to increase across most regions in the weak mitigation scenarios (ssp370 and ssp585), particularly over South and East Asia (up to 10 ppb by 2100) due to a combination of increases in air pollutant emissions, increases in global CH_4 abundances and climate change. Discrepancies exist in the regional surface O_3 response in ssp370 between individual CMIP6 models due to differences in the future response of chemistry, climate and biogenic precursor

https://doi.org/10.5194/acp-2019-1211
Preprint. Discussion started: 21 January 2020


Atmospheric Chemistry and Physics Discussions

emissions. Benefits to regional air quality from large reductions in surface O_3 are possible across all regions for scenarios that contain strong climate and air pollutant mitigation measures, including those targeting CH_4.

CMIP6 models predict surface $PM_{2.5}$ concentrations to decreases across all regions in both the middle-of-the-road (ssp245) and strong mitigation scenarios (ssp126) by up to 12 μg m^{-3} due to the reduction in anthropogenic aerosols and aerosol precursor emissions, yielding a benefit to regional air quality. Whereas for the weak climate and air pollutant mitigation scenario (ssp370), annual mean surface $PM_{2.5}$ is simulated to increase across a number of regions. Implementing mitigation measures specifically targeting NTCFs on top of the ssp370 scenario shows immediate improvements in $PM_{2.5}$ concentrations, restricting any changes to below present day values. The largest change in regional mean $PM_{2.5}$ concentrations, and also largest diversity across CMIP6 models, is predicted in ssp370 across South Asia, an area with already poor air quality. Disagreements in the prediction of future changes to regional surface $PM_{2.5}$ concentrations between individual CMIP6 models can mainly be attributed to differences in the aerosol schemes implemented within models, in particular the formation mechanisms of organic aerosols. Additionally, the strength of the climate change signal within models and how this can have important impacts on natural aerosol emissions leading to discrepancies between models.

The results from CMIP6 provide an opportunity to assess the simulation of historical and future changes in air pollutants within the latest generation of Earth system and climate models using up to date scenarios of future socio-economic development. Large changes in air pollutants were simulated over the historical period, primarily in response to changes in anthropogenic emissions. Future regional concentrations of air pollutants depend on the particular trajectory of climate and air pollutant mitigation that the world follows, with important consequences for regional air quality and human health. Substantial benefits can be achieved across most world regions by implementing measures to mitigate the extent of climate change, as well as from large reductions in air pollutants emissions, including CH_4 which is particularly important for controlling O_3. In future scenarios which do not mitigate climate change and air pollutant emissions, the regional concentrations of air pollutants are anticipated to increase. Important differences between individual CMIP6 models have been identified in terms of how they treat the interaction of chemistry, climate and natural precursor emissions in the future. Further research and understanding is necessary of these processes to improve the robustness of regional predictions of air pollutants on climate change timescales (decadal to centennial).

Data Availability

CMIP6 data is archived at the Earth System Grid Federation and is freely available to download. A list of the model datasets used in this study are provided in Table 1.

https://doi.org/10.5194/acp-2019-1211
Preprint. Discussion started: 21 January 2020

Author Contributions

S.T.T. conducted the analysis and wrote the paper with contributions from R.J.A. T.W. and J.Z. performed BCC-ESM1 simulations. L.E. and S.T. performed CESM2-WACCM simulations. P.N. and M.M. performed CNRM-ESM2-1 simulations. L.H. and V.N. performed GFDL-ESM4 simulations. S.B. and K.T. performed GISS-E2-1-H simulations. M.A and P.G. performed HadGEM3-GC31-LL simulations. T.T. performed MIROC6-ES2L simulations. D.N. performed MPI-ESM1.2-HAM simulations. D.O. and M.S. performed NorESM2-LM simulations. A.S. and F.M.O'C. performed UKESM1-0-LL simulations. All co-authors have been involved in providing comments and editing the manuscript.

Competing Interests

The author declares that there are no conflicts of interest.

Acknowledgements

S.T.T. and F.M.O'C. would like to acknowledge that support for this work came from the BEIS and DEFRA Met Office Hadley Centre Climate Programme (GA01101). S.T.T. would also like to acknowledge the UK-China Research and Innovation Partnership Fund through the Met Office Climate Science for Service Partnership (CSSP) China as part of the Newton Fund. FMO'C also acknowledge the EU Horizon 2020 Research Programme CRESCENDO project, grant agreement number 641816. T.T. was supported by the supercomputer system of the National Institute for Environmental Studies, Japan, and JSPS KAKENHI Grant Number JP19H05669. K.T. and S.B. acknowledge resources supporting this work were provided by the NASA High-End Computing (HEC) Program through the NASA Center for Climate Simulation (NCCS) at Goddard Space Flight Center.

For making their measurement data available to be used in this study we would like to acknowledge the providers who supplied their data to the GASSP database and TOAR database. David Neubauer acknowledges funding from the European Union's Horizon 2020 research and innovation programme project FORCeS under grant agreement No 821205 and a grant from the Deutsches Klimarechenzentrum (DKRZ) under project ID 1051.

References

Allen, R. J., Landuyt, W. and Rumbold, S. T.: An increase in aerosol burden and radiative effects in a warmer world, Nat. Clim. Chang., 6(3), 269–274, doi:10.1038/nclimate2827, 2016.

Allen, R. J., Turnock, S. T., Nabat, P., Neubauer, D., Lohmann, U., Olivié, D., Oshima, N., Michou, M., Wu, T., Zhang, J., Takemura, T., Schulz, M., Tsigaridis, K., Bauer, S. E., Emmons, L., Horowitz, L. W., Naik, V., Van Noije, T., Bergman, T., Lamarque, J.-F., Zanis, P., Tegen, I., Westervelt, D. M., Le Sager, P., Good, P., Shim, S., O'Connor, F. M., Akritidis, D., Georgoulias, A. K., Deushi, M., Sentman, L., Fujimori, S. and Collins, W. J.: Climate and air quality impacts due to mitigation of non-methane near-term climate forcers, submitted, 2019.

https://doi.org/10.5194/acp-2019-1211
Preprint. Discussion started: 21 January 2020

Apte, J. S., Marshall, J. D., Cohen, A. J. and Brauer, M.: Addressing Global Mortality from Ambient PM 2.5, Environ. Sci. Technol., 49, 8057–8066, doi:10.1021/acs.est.5b01236, 2015.

Archibald, A. T., Folberth, G., Wade, D. C. and Scott, D.: A world avoided: impacts of changes in anthropogenic emissions on the burden and effects of air pollutants in Europe and North America, Faraday Discuss., 200(0), 475–500, doi:10.1039/C7FD00004A, 2017.

Bauer, S. E. and Tsigaridis, K.: The end of the anthropogenic aerosol era?, submitted, 2019.

Bloomer, B. J., Stehr, J. W., Piety, C. A., Salawitch, R. J. and Dickerson, R. R.: Observed relationships of ozone air pollution with temperature and emissions, Geophys. Res. Lett., 36(9), 1–5, doi:10.1029/2009GL037308, 2009.

Boucher, O., Randall, P., Artaxo, P., Bretherton, C., Feingold, G., Forster, P., Kerminen, V.-M., Kondo, Y., Liao, H., Lohmann, U., Rasch, P., Satheesh, S. K., Sherwood, S., Stevens, B. and Zhang, X. Y.: Clouds and Aerosols. In: Climate Change 2013: The Physical Science Basis. Contribution of Working Group I to the Fifth Assessment Report of the Intergovernmental Panel on Climate Change, Cambridge University Press., 2013.

Buchard, V., Randles, C. A., da Silva, A. M., Darmenov, A., Colarco, P. R., Govindaraju, R., Ferrare, R., Hair, J., Beyersdorf, A. J., Ziemba, L. D., Yu, H., Buchard, V., Randles, C. A., Silva, A. M. da, Darmenov, A., Colarco, P. R., Govindaraju, R., Ferrare, R., Hair, J., Beyersdorf, A. J., Ziemba, L. D. and Yu, H.: The MERRA-2 Aerosol Reanalysis, 1980 Onward. Part II: Evaluation and Case Studies, J. Clim., 30(17), 6851–6872, doi:10.1175/JCLI-D-16-0613.1, 2017.

Butt, E. W., Turnock, S. T., Rigby, R., Reddington, C. L., Yoshioka, M., Johnson, J. S., Regayre, L. A., Pringle, K. J., Mann, G. W. and Spracklen, D. V.: Global and regional trends in particulate air pollution and attributable health burden over the past 50 years, Environ. Res. Lett., 12(10), doi:10.1088/1748-9326/aa87be, 2017.

Checa-Garcia, R., Hegglin, M. I., Kinnison, D., Plummer, D. A. and Shine, K. P.: Historical Tropospheric and Stratospheric Ozone Radiative Forcing Using the CMIP6 Database, Geophys. Res. Lett., 45(7), 3264–3273, doi:10.1002/2017GL076770, 2018.

Cohen, A. J., Brauer, M., Burnett, R., Anderson, H. R., Frostad, J., Estep, K., Balakrishnan, K., Brunekreef, B., Dandona, L., Dandona, R., Feigin, V., Freedman, G., Hubbell, B., Jobling, A., Kan, H., Knibbs, L., Liu, Y., Martin, R., Morawska, L., Pope, C. A., Shin, H., Straif, K., Shaddick, G., Thomas, M., van Dingenen, R., van Donkelaar, A., Vos, T., Murray, C. J. L. and Forouzanfar, M. H.: Estimates and 25-year trends of the global burden of disease attributable to ambient air pollution: an analysis of data from the Global Burden of Diseases Study 2015., Lancet (London, England), 389(10082), 1907–1918, doi:10.1016/S0140-6736(17)30505-6, 2017.

Colette, A., Andersson, C., Baklanov, A., Bessagnet, B., Brandt, J., Christensen, J. H., Doherty, R., Engardt, M., Geels, C., Giannakopoulos, C., Hedegaard, G. B., Katragkou, E., Langner, J., Lei, H., Manders, A., Melas, D., Meleux, F., Rouïl, L., Sofiev, M., Soares, J., Stevenson, D. S., Tombrou-Tzella, M., Varotsos, K. V and Young, P.: Is the ozone climate penalty robust in Europe?, Environ. Res. Lett., 10(8), 84015, doi:10.1088/1748-9326/10/8/084015, 2015.

Collins, J. W., Lamarque, J. F., Schulz, M., Boucher, O., Eyring, V., Hegglin, I. M., Maycock, A., Myhre, G., Prather, M., Shindell, D. and Smith, J. S.: AerChemMIP: Quantifying the effects of chemistry and aerosols in CMIP6, Geosci. Model Dev., 10(2), 585–607, doi:10.5194/gmd-10-585-2017, 2017.

Danabasoglu, G.: NCAR CESM2-WACCM model output prepared for CMIP6 AerChemMIP, , doi:10.22033/ESGF/CMIP6.10023, 2019a.

Danabasoglu, G.: NCAR CESM2-WACCM model output prepared for CMIP6 CMIP, , doi:10.22033/ESGF/CMIP6.10024, 2019b.

Danabasoglu, G.: NCAR CESM2-WACCM model output prepared for CMIP6 ScenarioMIP, , doi:10.22033/ESGF/CMIP6.10026, 2019c.

Daskalakis, N., Tsigaridis, K., Myriokefalitakis, S., Fanourgakis, G. S. and Kanakidou, M.: Large gain in air quality compared to an alternative anthropogenic emissions scenario, Atmos. Chem. Phys., 16(15), 9771–9784, doi:10.5194/acp-16-9771-2016, 2016.

Doherty, R. M., Wild, O., Shindell, D. T., Zeng, G., MacKenzie, I. A., Collins, W. J., Fiore, A. M., Stevenson, D. S., Dentener, F. J., Schultz,

https://doi.org/10.5194/acp-2019-1211
Preprint. Discussion started: 21 January 2020

M. G., Hess, P., Derwent, R. G. and Keating, T. J.: Impacts of climate change on surface ozone and intercontinental ozone pollution: A multi-model study, J. Geophys. Res. Atmos., 118(9), 3744–3763, doi:10.1002/jgrd.50266, 2013.

Dunne, J. P.: The GFDL Earth System Model version 4.1 (GFDL-ESM4.1): Model description and simulation characteristics, J. Adv. Model. Earth Syst., In Prep, 2019.

Emmons, L. K., Orlando, J. J., Tyndall, G., Schwantes, R. H., Kinnison, D., Lamarque, J.-F., Marsh, D., Mills, M., Tilmes, S., Buchholtz, R. R., Gettelman, A., Garcia, R., Simpson, I., Blake, D. R. and Pétron, G.: The Chemistry Mechanism in the Community Earth System Model verson 2 (CESM2), J. Adv. Model. Earth Syst., submitted, 2019.

Eyring, V., Bony, S., Meehl, G. A., Senior, C. A., Stevens, B., Stouffer, R. J. and Taylor, K. E.: Overview of the Coupled Model Intercomparison Project Phase 6 (CMIP6) experimental design and organization, Geosci. Model Dev., 9(5), 1937–1958, doi:10.5194/gmd-9-1937-2016, 2016.

Fagerli, H. and Aas, W.: Trends of nitrogen in air and precipitation: Model results and observations at EMEP sites in Europe, 1980–2003, Environ. Pollut., 154(3), 448–461 [online] Available from: http://www.sciencedirect.com/science/article/pii/S0269749108000523 (Accessed 9 December 2013), 2008.

Fiore, A. M., Naik, V., Spracklen, D. V, Steiner, A., Unger, N., Prather, M., Bergmann, D., Cameron-Smith, P. J., Cionni, I., Collins, W. J., Dalsøren, S., Eyring, V., Folberth, G. a, Ginoux, P., Horowitz, L. W., Josse, B., Lamarque, J.-F., MacKenzie, I. a, Nagashima, T., O'Connor, F. M., Righi, M., Rumbold, S. T., Shindell, D. T., Skeie, R. B., Sudo, K., Szopa, S., Takemura, T. and Zeng, G.: Global air quality and climate., Chem. Soc. Rev., 41(19), 6663–83, doi:10.1039/c2cs35095e, 2012.

Forster, P. M., Maycock, A. C., McKenna, C. M. and Smith, C. J.: Latest climate models confirm need for urgent mitigation, Nat. Clim. Chang., 1–4, doi:10.1038/s41558-019-0660-0, 2019.

Fowler, D., Pilegaard, K., Sutton, M. A., Ambus, P., Raivonen, M., Duyzer, J., Simpson, D., Fagerli, H., Fuzzi, S., Schjoerring, J. K., Granier, C., Neftel, A., Isaksen, I. S. A., Laj, P., Maione, M., Monks, P. S., Burkhardt, J., Daemmgen, U., Neirynck, J., Personne, E., Wichink-Kruit, R., Butterbach-Bahl, K., Flechard, C., Tuovinen, J. P., Coyle, M., Gerosa, G., Loubet, B., Altimir, N., Gruenhage, L., Ammann, C., Cieslik, S., Paoletti, E., Mikkelsen, T. N., Ro-Poulsen, H., Cellier, P., Cape, J. N., Horváth, L., Loreto, F., Niinemets, Ü., Palmer, P. I., Rinne, J., Misztal, P., Nemitz, E., Nilsson, D., Pryor, S., Gallagher, M. W., Vesala, T., Skiba, U., Brüggemann, N., Zechmeister-Boltenstern, S., Williams, J., O'Dowd, C., Facchini, M. C., de Leeuw, G., Flossman, A., Chaumerliac, N. and Erisman, J. W.: Atmospheric composition change: Ecosystems–Atmosphere interactions, Atmos. Environ., 43(33), 5193–5267, doi:10.1016/j.atmosenv.2009.07.068, 2009.

Gettelman, A., Truesdale, J. E., Bacmeister, J. T., Caldwell, P. M., Neale, R. B., Bogenschutz, P. A. and Simpson, I. R.: The Whole Atmosphere Community Climate Model Version 6 (WACCM6), J. Geophys. Res. Atmos., in press, 2019.

Gidden, M. J., Riahi, K., Smith, S. J., Fujimori, S., Luderer, G., Kriegler, E., van Vuuren, D. P., van den Berg, M., Feng, L., Klein, D., Calvin, K., Doelman, J. C., Frank, S., Fricko, O., Harmsen, M., Hasegawa, T., Havlik, P., Hilaire, J., Hoesly, R., Horing, J., Popp, A., Stehfest, E. and Takahashi, K.: Global emissions pathways under different socioeconomic scenarios for use in CMIP6: a dataset of harmonized emissions trajectories through the end of the century, Geosci. Model Dev., 12(4), 1443–1475, doi:10.5194/gmd-12-1443-2019, 2019.

Glotfelty, T., He, J. and Zhang, Y.: Impact of future climate policy scenarios on air quality and aerosol-cloud interactions using an advanced version of CESM/CAM5: Part I. model evaluation for the current decadal simulations, Atmos. Environ., 152, 222–239, doi:10.1016/J.ATMOSENV.2016.12.035, 2017.

Good, P.: MOHC HadGEM3-GC31-LL model output prepared for CMIP6 ScenarioMIP, , doi:10.22033/ESGF/CMIP6.10845, 2019.

Good, P., Sellar, A., Tang, Y., Rumbold, S., Ellis, R., Kelley, D., Kuhlbrodt, T. and Walton, J.: MOHC UKESM1.0-LL model output

https://doi.org/10.5194/acp-2019-1211
Preprint. Discussion started: 21 January 2020

prepared for CMIP6 ScenarioMIP, , doi:10.22033/ESGF/CMIP6.1567, 2019.

Griffiths, P., Archibald, A. T., Zeng, G., Zanis, P., Hassler, B., O'Connor, F. M., Turnock, S. T., Naik, V., Young, P., Wild, O., Keeble, J., Shin, Y., Ziemke, J. R., Galbally, I., Tarasick, D., Jingxian., L., Omid, M. and Murray, L. T.: Tropospheric Ozone in CMIP6 Simulations, Submitted, 2019.

Hajima, T. and Kawamiya, M.: MIROC MIROC-ES2L model output prepared for CMIP6 CMIP, , doi:10.22033/ESGF/CMIP6.902, 2019.

Hajima, T., Watanabe, M., Yamamoto, A., Tatebe, H., Noguchi, A., Abe, M., Ohgaito, R., Ito, A., Yamazaki, D., Ito, A., Takata, K., Ogochi, K. and Watanabe, S.: Description of the MIROC-ES2L Earth system model and evaluation of its climate – biogeochemical processes and feedbacks, Geosci. Model Dev. Discuss., 5(October), 2019.

Hoesly, R. M., Smith, S. J., Feng, L., Klimont, Z., Janssens-Maenhout, G., Pitkanen, T., Seibert, J. J., Vu, L., Andres, R. J., Bolt, R. M., Bond, T. C., Dawidowski, L., Kholod, N., Kurokawa, J., Li, M., Liu, L., Lu, Z., Moura, M. C. P., O'Rourke, P. R. and Zhang, Q.: Historical (1750–2014) anthropogenic emissions of reactive gases and aerosols from the Community Emissions Data System (CEDS), Geosci. Model Dev., 11(1), 369–408, doi:10.5194/gmd-11-369-2018, 2018.

Horowitz, L. W.: The GFDL Global Atmospheric Chemistry-Climate Model AM4.1: Model Description and Simulation Characteristics, J. Adv. Model. Earth Syst., In Prep, 2019.

Horowitz, L. W., Naik, V., Sentman, L. T., Paulot, F., Blanton, C., McHugh, C., Radhakrishnan, A., Rand, K., Ginoux, P. and Paynter, D. J.: NOAA-GFDL GFDL-ESM4 model output prepared for CMIP6 AerChemMIP ssp370-lowNTCF, , doi:10.22033/ESGF/CMIP6.8693, 2018.

Isaksen, I. S. A., Granier, C., Myhre, G., Berntsen, T. K., Dalsøren, S. B., Gauss, M., Klimont, Z., Benestad, R., Bousquet, P., Collins, W., Cox, T., Eyring, V., Fowler, D., Fuzzi, S., Jöckel, P., Laj, P., Lohmann, U., Maione, M., Monks, P., Prevot, A. S. H., Raes, F., Richter, A., Rognerud, B., Schulz, M., Shindell, D., Stevenson, D. S., Storelvmo, T., Wang, W.-C., van Weele, M., Wild, M. and Wuebbles, D.: Atmospheric composition change: Climate–Chemistry interactions, Atmos. Environ., 43(33), 5138–5192 [online] Available from: http://www.sciencedirect.com/science/article/pii/S1352231009006943 (Accessed 9 December 2013), 2009.

Jacob, D. J. and Winner, D. a.: Effect of climate change on air quality, Atmos. Environ., 43(1), 51–63, doi:10.1016/j.atmosenv.2008.09.051, 2009.

John, J. G., Blanton, C., McHugh, C., Nikonov, S., Radhakrishnan, A., Rand, K., Vahlenkamp, H., Zadeh, N. T., Gauthier, P. P. G., Ginoux, P., Harrison, M., Horowitz, L. W., Malyshev, S., Naik, V., Paynter, D. J., Ploshay, J., Silvers, L., Stock, C., Winton, M., Zeng, Y. and Dunne, J. P.: NOAA-GFDL GFDL-ESM4 model output prepared for CMIP6 ScenarioMIP, , doi:10.22033/ESGF/CMIP6.1414, 2018.

Karset, I. H. H., Berntsen, T. K., Storelvmo, T., Alterskjær, K., Grini, A., Olivié, D., Kirkevåg, A., Seland, Ø., Iversen, T. and Schulz, M.: Strong impacts on aerosol indirect effects from historical oxidant changes, Atmos. Chem. Phys., 18(10), 7669–7690, doi:10.5194/acp-18-7669-2018, 2018.

Kirkevåg, A., Grini, A., Olivié, D., Seland, Ø., Alterskjær, K., Hummel, M., Karset, I. H. H., Lewinschal, A., Liu, X., Makkonen, R., Bethke, I., Griesfeller, J., Schulz, M. and Iversen, T.: A production-tagged aerosol module for Earth system models, OsloAero5.3 – extensions and updates for CAM5.3-Oslo, Geosci. Model Dev., 11(10), 3945–3982, doi:10.5194/gmd-11-3945-2018, 2018.

Kirtman, B., Power, S. B., Adedoyin, J. A., Boer, G. J., Bojariu, R., Camilloni, I., Doblas-Reyes, F. J., Fiore, A. M., Kimoto, M., Meehl, G. A., Prather, M., Sarr, A., Schar, C., Sutton, R., van Oldenborgh, G. J., Vecchi, G. and Wang, H. J.: Near-term Climate Change: Projections and Predictability. In: Climate Change 2013: The Physical Science Basis. Contribution of Working Group I to the Fifth Assessment Report of the Intergovernmental Panel on Climate Change, edited by T. F. Stocker, D. Qin, G.-K. Plattner, M. Tignore, S. K. Allen, J. Boschung, A. Nauels, Y. Xia, V. Bex, and P. M. Midgley, Cambridge University Press, Cambridge, United Kingdom and New York, NY, USA., 2013.

https://doi.org/10.5194/acp-2019-1211
Preprint. Discussion started: 21 January 2020

Atmospheric Chemistry and Physics Discussions

Krasting, J. P., John, J. G., Blanton, C., McHugh, C., Nikonov, S., Radhakrishnan, A., Rand, K., Zadeh, N. T., Balaji, V., Durachta, J., Dupuis, C., Menzel, R., Robinson, T., Underwood, S., Vahlenkamp, H., Dunne, K. A., Gauthier, P. P. G., Ginoux, P., Griffies, S. M., Hallberg, R., Harrison, M., Hurlin, W., Malyshev, S., Naik, V., Paulot, F., Paynter, D. J., Ploshay, J., Schwarzkopf, D. M., Seman, C. J., Silvers, L., Wyman, B., Zeng, Y., Adcroft, A., Dunne, J. P., Guo, H., Held, I. M., Horowitz, L. W., Milly, P. C. D., Shevliakova, E., Stock, C., Winton, M. and Zhao, M.: NOAA-GFDL GFDL-ESM4 model output prepared for CMIP6 CMIP, , doi:10.22033/ESGF/CMIP6.1407, 2018.

Kuhlbrodt, T., Jones, C. G., Sellar, A., Storkey, D., Blockley, E., Stringer, M., Hill, R., Graham, T., Ridley, J., Blaker, A., Calvert, D., Copsey, D., Ellis, R., Hewitt, H., Hyder, P., Ineson, S., Mulcahy, J., Siahaan, A. and Walton, J.: The Low-Resolution Version of HadGEM3 GC3.1: Development and Evaluation for Global Climate, J. Adv. Model. Earth Syst., 10(11), 2865–2888, doi:10.1029/2018MS001370, 2018.

Lamarque, J.-F., Shindell, D. T., Josse, B., Young, P. J., Cionni, I., Eyring, V., Bergmann, D., Cameron-Smith, P., Collins, W. J., Doherty, R., Dalsoren, S., Faluvegi, G., Folberth, G., Ghan, S. J., Horowitz, L. W., Lee, Y. H., MacKenzie, I. A., Nagashima, T., Naik, V., Plummer, D., Righi, M., Rumbold, S. T., Schulz, M., Skeie, R. B., Stevenson, D. S., Strode, S., Sudo, K., Szopa, S., Voulgarakis, A. and Zeng, G.: The Atmospheric Chemistry and Climate Model Intercomparison Project (ACCMIP): overview and description of models, simulations and climate diagnostics, Geosci. Model Dev., 6(1), 179–206, doi:10.5194/gmd-6-179-2013, 2013.

Leibensperger, E. M., Mickley, L. J., Jacob, D. J., Chen, W.-T., Seinfeld, J. H., Nenes, a., Adams, P. J., Streets, D. G., Kumar, N. and Rind, D.: Climatic effects of 1950–2050 changes in US anthropogenic aerosols – Part 2: Climate response, Atmos. Chem. Phys., 12(7), 3349–3362, doi:10.5194/acp-12-3349-2012, 2012.

Lelieveld, J., Evans, J. S., Fnais, M., Giannadaki, D. and Pozzer, a: The contribution of outdoor air pollution sources to premature mortality on a global scale., Nature, 525(7569), 367–71, doi:10.1038/nature15371, 2015.

Malley, C. S., Henze, D. K., Kuylenstierna, J. C. I., Vallack, H. W., Davila, Y., Anenberg, S. C., Turner, M. C. and Ashmore, M. R.: Updated Global Estimates of Respiratory Mortality in Adults ≥30 Years of Age Attributable to Long-Term Ozone Exposure, Environ. Health Perspect., 125(8), 87021, doi:10.1289/EHP1390, 2017.

van Marle, M. J. E., Kloster, S., Magi, B. I., Marlon, J. R., Daniau, A.-L., Field, R. D., Arneth, A., Forrest, M., Hantson, S., Kehrwald, N. M., Knorr, W., Lasslop, G., Li, F., Mangeon, S., Yue, C., Kaiser, J. W. and van der Werf, G. R.: Historic global biomass burning emissions for CMIP6 (BB4CMIP) based on merging satellite observations with proxies and fire models (1750–2015), Geosci. Model Dev., 10(9), 3329–3357, doi:10.5194/gmd-10-3329-2017, 2017.

Mulcahy, J. P., Turnock, S. T., Abraham, N. L., Bellouin, N., Browse, J., Carslaw, K. S., Dalvi, M., Folberth, G. A., Grosvenor, D., Hardacre, C., Johnson, C., Johnson, B., Jones, A., Jones, C., Kipling, Z., Mann, G. W., O'Connor, F. M., Palmieri, J., Povey, A., Reddington, C. L., Richardson, M., Sellar, A., Scott, C. E., Stier, P., Woodhouse, M. T., Woodward, S. and Yool, A.: Description and evaluation of aerosol in UKESM1 and HadGEM-GC3.1 CMIP6 historical simulations, submitted, 2019.

Myhre, G., Shindell, D., Breon, F.-M., Collins, W., Fuglestvedt, J., Huang, J., Koch, D., Lamarque, J.-F., Lee, D., Mendoza, B., Nakajima, T., Robock, A., Stephens, G., Takemura, T. and Zhang, H.: Anthropogenic and Natural Radiative Forcing. In: Climate Change 2013: The Physical Science Basis. Contribution of Working Group I to the Fifth Assessment Report of the Intergovernemental Panel on Cliamte Change, edited by T. F. Stocker, D. Qin, G.-K. Plattner, M. Tignore, S. K. Allen, J. Boschung, A. Nauels, Y. Xia, V. Bex, and P. M. Midgley, Cambridge University Press, Cambridge, United Kingdom and New York, NY, USA., 2013.

NASA Goddard Institute For Space Studies (NASA/GISS): NASA-GISS GISS-E2.1H model output prepared for CMIP6 CMIP, , doi:10.22033/ESGF/CMIP6.1421, 2018.

https://doi.org/10.5194/acp-2019-1211
Preprint. Discussion started: 21 January 2020

Neubauer, D., Ferrachat, S., Siegenthaler-Le Drian, C., Stoll, J., Folini, D. S., Tegen, I., Wieners, K.-H., Mauritsen, T., Stemmler, I., Barthel, S., Bey, I., Daskalakis, N., Heinold, B., Kokkola, H., Partridge, D., Rast, S., Schmidt, H., Schutgens, N., Stanelle, T., Stier, P., Watson-Parris, D. and Lohmann, U.: HAMMOZ-Consortium MPI-ESM1.2-HAM model output prepared for CMIP6 AerChemMIP, , doi:10.22033/ESGF/CMIP6.1621, 2019.

Norwegian Climate Center (NCC): NCC NorESM2-LM model output prepared for CMIP6 CMIP historical, [online] Available from: http://cera-www.dkrz.de/WDCC/meta/CMIP6/CMIP6.CMIP.NCC.NorESM2-LM.historical, 2018.

O'Neill, B. C., Kriegler, E., Riahi, K., Ebi, K. L., Hallegatte, S., Carter, T. R., Mathur, R. and van Vuuren, D. P.: A new scenario framework for climate change research: the concept of shared socioeconomic pathways, Clim. Change, 122(3), 387–400, doi:10.1007/s10584-013-0905-2, 2014.

O'Neill, B. C., Tebaldi, C., van Vuuren, D. P., Eyring, V., Friedlingstein, P., Hurtt, G., Knutti, R., Kriegler, E., Lamarque, J.-F., Lowe, J., Meehl, G. A., Moss, R., Riahi, K. and Sanderson, B. M.: The Scenario Model Intercomparison Project (ScenarioMIP) for CMIP6, Geosci. Model Dev., 9(9), 3461–3482, doi:10.5194/gmd-9-3461-2016, 2016.

Pozzer, A., Meij, A. De, Pringle, K. J., Tost, H., Doering, U. M., Aardenne, J. Van and Lelieveld, J.: Distributions and regional budgets of aerosols and their precursors simulated with the EMAC chemistry-climate model, Atmos. Chem. Phys., 12, 961–987, doi:10.5194/acp-12-961-2012, 2012.

Provençal, S., Buchard, V., da Silva, A. M., Leduc, R., Barrette, N., Elhacham, E. and Wang, S.-H.: Evaluation of PM2.5 surface concentration simulated by Version 1 of the NASA's MERRA Aerosol Reanalysis over Israel and Taiwan., Aerosol air Qual. Res., 17(1), 253–261, doi:10.4209/aaqr.2016.04.0145, 2017.

Randles, C. A., da Silva, A. M., Buchard, V., Colarco, P. R., Darmenov, A., Govindaraju, R., Smirnov, A., Holben, B., Ferrare, R., Hair, J., Shinozuka, Y., Flynn, C. J., Randles, C. A., Silva, A. M. da, Buchard, V., Colarco, P. R., Darmenov, A., Govindaraju, R., Smirnov, A., Holben, B., Ferrare, R., Hair, J., Shinozuka, Y. and Flynn, C. J.: The MERRA-2 Aerosol Reanalysis, 1980 Onward. Part I: System Description and Data Assimilation Evaluation, J. Clim., 30(17), 6823–6850, doi:10.1175/JCLI-D-16-0609.1, 2017.

Rao, S., Klimont, Z., Leitao, J., Riahi, K., Van Dingenen, R., Reis, L. A., Calvin, K., Dentener, F., Drouet, L., Fujimori, S., Harmsen, M., Luderer, G., Heyes, C., Strefler, J., Tavoni, M. and Van Vuuren, D. P.: A multi-model assessment of the co-benefits of climate mitigation for global air quality, Environ. Res. Lett., 11(12), 124013, doi:10.1088/1748-9326/11/12/124013, 2016.

Rao, S., Klimont, Z., Smith, S. J., Dingenen, R. Van, Dentener, F., Bouwman, L., Riahi, K., Amann, M., Bodirsky, B. L., Van Vuuren, D. P., Reis, L. A., Calvin, K., Drouet, L., Fricko, O., Fujimori, S., Gernaat, D., Havlik, P., Harmsen, M., Hasegawa, T., Heyes, C., Hilaire, J., Luderer, G., Masui, T., Stehfest, E., Strefler, J., Van Der Sluis, S. and Tavoni, M.: Future air pollution in the Shared Socio-economic Pathways, Glob. Environ. Chang., 42, 346–358, doi:10.1016/j.gloenvcha.2016.05.012, 2017.

Rasmussen, D. J., Hu, J., Mahmud, A. and Kleeman, J. M.: The Ozone Climate Penalty: past, present and future, Environ. Sci. Technol., 47(24), 14258–14266, doi:10.1109/TMI.2012.2196707.Separate, 2013.

Reddington, C. L., Carslaw, K. S., Stier, P., Schutgens, N., Coe, H., Liu, D., Allan, J., Browse, J., Pringle, K. J., Lee, L. A., Yoshioka, M., Johnson, J. S., Regayre, L. A., Spracklen, D. V., Mann, G. W., Clarke, A., Hermann, M., Henning, S., Wex, H., Kristensen, T. B., Leaitch, W. R., Pöschl, U., Rose, D., Andreae, M. O., Schmale, J., Kondo, Y., Oshima, N., Schwarz, J. P., Nenes, A., Anderson, B., Roberts, G. C., Snider, J. R., Leck, C., Quinn, P. K., Chi, X., Ding, A., Jimenez, J. L. and Zhang, Q.: The global aerosol synthesis and science project (GASSP): Measurements and modeling to reduce uncertainty, Bull. Am. Meteorol. Soc., 98(9), 1857–1877, doi:10.1175/BAMS-D-15-00317.1, 2017.

Reis, L. A., Drouet, L., van Dingenen, R. and Emmerling, J.: Future global air quality indices under different socioeconomic and climate

https://doi.org/10.5194/acp-2019-1211
Preprint. Discussion started: 21 January 2020

assumptions, Sustain., 10(10), 1–27, doi:10.3390/su10103645, 2018.

Riahi, K., Van Vuuren, D. P., Kriegler, E., Edmonds, J., O 'neill, B. C., Fujimori, S., Bauer, N., Calvin, K., Dellink, R., Fricko, O., Lutz, W., Popp, A., Cuaresma, J. C., Kc, S., Leimbach, M., Jiang, L., Kram, T., Rao, S., Emmerling, J., Ebi, K., Hasegawa, T., Havlik, P., Humpenöder, F., Aleluia, L., Silva, D., Smith, S., Stehfest, E., Bosetti, V., Eom, J., Gernaat, D., Masui, T., Rogelj, J., Strefler, J., Drouet, L., Krey, V., Luderer, G., Harmsen, M., Takahashi, K., Baumstark, L., Doelman, J. C., Kainuma, M., Klimont, Z., Marangoni, G., Lotze-Campen, H., Obersteiner, M., Tabeau, A. and Tavoni, M.: The Shared Socioeconomic Pathways and their energy, land use, and greenhouse gas emissions implications: An overview, Glob. Environ. Chang., 42, 153–168, doi:10.1016/j.gloenvcha.2016.05.009, 2017.

Ridley, J., Menary, M., Kuhlbrodt, T., Andrews, M. and Andrews, T.: MOHC HadGEM3-GC31-LL model output prepared for CMIP6 CMIP, , doi:10.22033/ESGF/CMIP6.419, 2018.

Schultz, M. G., Schröder, S., Lyapina, O., Cooper, O., Galbally, I., Petropavlovskikh, I., Von Schneidemesser, E., Tanimoto, H., Elshorbany, Y., Naja, M., Seguel, R., Dauert, U., Eckhardt, P., Feigenspahn, S., Fiebig, M., Hjellbrekke, A.-G., Hong, Y.-D., Christian Kjeld, P., Koide, H., Lear, G., Tarasick, D., Ueno, M., Wallasch, M., Baumgardner, D., Chuang, M.-T., Gillett, R., Lee, M., Molloy, S., Moolla, R., Wang, T., Sharps, K., Adame, J. A., Ancellet, G., Apadula, F., Artaxo, P., Barlasina, M., Bogucka, M., Bonasoni, P., Chang, L., Colomb, A., Cuevas, E., Cupeiro, M., Degorska, A., Ding, A., Fröhlich, M., Frolova, M., Gadhavi, H., Gheusi, F., Gilge, S., Gonzalez, M. Y., Gros, V., Hamad, S. H., Helmig, D., Henriques, D., Hermansen, O., Holla, R., Huber, J., Im, U., Jaffe, D. A., Komala, N., Kubistin, D., Lam, K.-S., Laurila, T., Lee, H., Levy, I., Mazzoleni, C., Mazzoleni, L., McClure-Begley, A., Mohamad, M., Murovic, M., Navarro-Comas, M., Nicodim, F., Parrish, D., Read, K. A., Reid, N., Ries, L., Saxena, P., Schwab, J. J., Scorgie, Y., Senik, I., Simmonds, P., Sinha, V., Skorokhod, A., Spain, G., Spangl, W., Spoor, R., Springston, S. R., Steer, K., Steinbacher, M., Suharguniyawan, E., Torre, P., Trickl, T., Weili, L., Weller, R., Xu, X., Xue, L. and Zhiqiang, M.: Tropospheric Ozone Assessment Report: Database and Metrics Data of Global Surface Ozone Observations, Elem Sci Anth, 5(0), 58, doi:10.1525/elementa.244, 2017.

Seferian, R.: CNRM-CERFACS CNRM-ESM2-1 model output prepared for CMIP6 CMIP, , doi:10.22033/ESGF/CMIP6.1391, 2018.

Seferian, R.: CNRM-CERFACS CNRM-ESM2-1 model output prepared for CMIP6 AerChemMIP, , doi:10.22033/ESGF/CMIP6.1389, 2019.

Séférian, R., Nabat, P., Michou, M., Saint-Martin, D., Voldoire, A., Colin, J., Decharme, B., Delire, C., Berthet, S., Chevallier, M., Sénési, S., Franchisteguy, L., Vial, J., Mallet, M., Joetzjer, E., Geoffroy, O., Guérémy, J., Moine, M., Msadek, R., Ribes, A., Rocher, M., Roehrig, R., Salas-y-Mélia, D., Sanchez, E., Terray, L., Valcke, S., Waldman, R., Aumont, O., Bopp, L., Deshayes, J., Éthé, C. and Madec, G.: Evaluation of CNRM Earth System Model, CNRM-ESM2-1: Role of Earth System Processes in Present-Day and Future Climate, J. Adv. Model. Earth Syst., 2019MS001791, doi:10.1029/2019MS001791, 2019.

Sellar, A. A., Jones, C. G., Mulcahy, J., Tang, Y., Yool, A., Wiltshire, A., O'Connor, F. M., Stringer, M., Hill, R., Palmieri, J., Woodward, S., Mora, L., Kuhlbrodt, T., Rumbold, S., Kelley, D. I., Ellis, R., Johnson, C. E., Walton, J., Abraham, N. L., Andrews, M. B., Andrews, T., Archibald, A. T., Berthou, S., Burke, E., Blockley, E., Carslaw, K., Dalvi, M., Edwards, J., Folberth, G. A., Gedney, N., Griffiths, P. T., Harper, A. B., Hendry, M. A., Hewitt, A. J., Johnson, B., Jones, A., Jones, C. D., Keeble, J., Liddicoat, S., Morgenstern, O., Parker, R. J., Predoi, V., Robertson, E., Siahaan, A., Smith, R. S., Swaminathan, R., Woodhouse, M. T., Zeng, G. and Zerroukat, M.: UKESM1: Description and evaluation of the UK Earth System Model, J. Adv. Model. Earth Syst., 2019MS001739, doi:10.1029/2019MS001739, 2019.

Shen, L., Mickley, L. J. and Murray, L. T.: Influence of 2000–2050 climate change on particulate matter in the United States: results from a new statistical model, Atmos. Chem. Phys., 17(6), 4355–4367, doi:10.5194/acp-17-4355-2017, 2017.

Silva, R. a, West, J. J., Zhang, Y., Anenberg, S. C., Lamarque, J.-F., Shindell, D. T., Collins, W. J., Dalsoren, S., Faluvegi, G., Folberth, G., Horowitz, L. W., Nagashima, T., Naik, V., Rumbold, S., Skeie, R., Sudo, K., Takemura, T., Bergmann, D., Cameron-Smith, P., Cionni, I.,

https://doi.org/10.5194/acp-2019-1211
Preprint. Discussion started: 21 January 2020

Doherty, R. M., Eyring, V., Josse, B., MacKenzie, I. a, Plummer, D., Righi, M., Stevenson, D. S., Strode, S., Szopa, S. and Zeng, G.: Global premature mortality due to anthropogenic outdoor air pollution and the contribution of past climate change, Environ. Res. Lett., 8, 34005, doi:10.1088/1748-9326/8/3/034005, 2013.

Silva, R. A., West, J. J., Lamarque, J. F., Shindell, D. T., Collins, W. J., Faluvegi, G., Folberth, G. A., Horowitz, L. W., Nagashima, T., Naik, V., Rumbold, S. T., Sudo, K., Takemura, T., Bergmann, D., Cameron-Smith, P., Doherty, R. M., Josse, B., MacKenzie, I. A., Stevenson, D. S. and Zeng, G.: Future global mortality from changes in air pollution attributable to climate change, Nat. Clim. Chang., 7(9), 647–651, doi:10.1038/nclimate3354, 2017.

Solazzo, E., Bianconi, R., Hogrefe, C., Curci, G., Tuccella, P., Alyuz, U., Balzarini, A., Baró, R., Bellasio, R., Bieser, J., Brandt, J., Christensen, J. H., Colette, A., Francis, X., Fraser, A., Vivanco, M. G., Jiménez-Guerrero, P., Im, U., Manders, A., Nopmongcol, U., Kitwiroon, N., Pirovano, G., Pozzoli, L., Prank, M., Sokhi, R. S., Unal, A., Yarwood, G. and Galmarini, S.: Evaluation and error apportionment of an ensemble of atmospheric chemistry transport modeling systems: multivariable temporal and spatial breakdown, Atmos. Chem. Phys., 17(4), 3001–3054, doi:10.5194/acp-17-3001-2017, 2017.

Tachiiri, K. and Kawamiya, M.: MIROC MIROC-ES2L model output prepared for CMIP6 ScenarioMIP, , doi:10.22033/ESGF/CMIP6.936, 2019.

Takemura, T.: Distributions and Climate Effects of Atmospheric Aerosols from the preindustrial era to 2100 along Representative Concentration Pathways (RCPs) simulated using the GLobal Aerosol Model SPRINTARS, Atmos. Chem. Phys., 12, 11555–11572 [online] Available from: http://www.atmos-chem-phys.net/12/11555/2012/acp-12-11555-2012.pdf, 2012.

Tang, Y., Rumbold, S., Ellis, R., Kelley, D., Mulcahy, J., Sellar, A., Walton, J. and Jones, C.: MOHC UKESM1.0-LL model output prepared for CMIP6 CMIP, , doi:10.22033/ESGF/CMIP6.1569, 2019.

Taylor, K. E., Stouffer, R. J. and Meehl, G. A.: An Overview of CMIP5 and the Experiment Design, Bull. Am. Meteorol. Soc., 93(4), 485–498, doi:10.1175/BAMS-D-11-00094.1, 2012.

Tegen, I., Neubauer, D., Ferrachat, S., Siegenthaler-Le Drian, C., Bey, I., Schutgens, N., Stier, P., Watson-Parris, D., Stanelle, T., Schmidt, H., Rast, S., Kokkola, H., Schultz, M., Schroeder, S., Daskalakis, N., Barthel, S., Heinold, B. and Lohmann, U.: The global aerosol–climate model ECHAM6.3–HAM2.3 – Part 1: Aerosol evaluation, Geosci. Model Dev., 12(4), 1643–1677, doi:10.5194/gmd-12-1643-2019, 2019.

Tilmes, S., Hodzic, A., Emmons, L. K., Mills, M. J., Gettelman, A., Kinnison, D. E., Park, M., Lamarque, J. -F., Vitt, F., Shrivastava, M., Campuzano Jost, P., Jimenez, J. and Liu, X.: Climate forcing and trends of organic aerosols in the Community Earth System Model (CESM2), J. Adv. Model. Earth Syst., 2019MS001827, doi:10.1029/2019MS001827, 2019.

Tørseth, K., Aas, W., Breivik, K., Fjæraa, a. M., Fiebig, M., Hjellbrekke, a. G., Lund Myhre, C., Solberg, S. and Yttri, K. E.: Introduction to the European Monitoring and Evaluation Programme (EMEP) and observed atmospheric composition change during 1972–2009, Atmos. Chem. Phys., 12(12), 5447–5481, doi:10.5194/acp-12-5447-2012, 2012.

Turnock, S. T., Butt, E. W., Richardson, T. B., Mann, G. W., Reddington, C. L., Forster, P. M., Haywood, J., Crippa, M., Janssens-Maenhout, G., Johnson, C. E., Bellouin, N., Carslaw, K. S. and Spracklen, D. V: The impact of European legislative and technology measures to reduce air pollutants on air quality, human health and climate, Environ. Res. Lett., 11(2), 24010, doi:10.1088/1748-9326/11/2/024010, 2016.

Turnock, S. T., Wild, O., Sellar, A. and O'Connor, F. M.: 300 years of tropospheric ozone changes using CMIP6 scenarios with a parameterised approach, Atmos. Environ., 213, 686–698, doi:10.1016/J.ATMOSENV.2019.07.001, 2019.

United Nations: Paris Agreement, 2016.

Voldoire, A.: CNRM-CERFACS CNRM-ESM2-1 model output prepared for CMIP6 ScenarioMIP, , doi:10.22033/ESGF/CMIP6.1395, 2019.

https://doi.org/10.5194/acp-2019-1211
Preprint. Discussion started: 21 January 2020

van Vuuren, D. P., Kriegler, E., O'Neill, B. C., Ebi, K. L., Riahi, K., Carter, T. R., Edmonds, J., Hallegatte, S., Kram, T., Mathur, R. and Winkler, H.: A new scenario framework for Climate Change Research: scenario matrix architecture, Clim. Change, 122(3), 373–386, doi:10.1007/s10584-013-0906-1, 2014.

Westervelt, D. M., Horowitz, L. W., Naik, V., Tai, A. P. K., Fiore, A. M. and Mauzerall, D. L.: Quantifying PM2.5-meteorology sensitivities in a global climate model, Atmos. Environ., 142, 43–56, doi:10.1016/J.ATMOSENV.2016.07.040, 2016.

Wild, O., Fiore, A. M., Shindell, D. T., Doherty, R. M., Collins, W. J., Dentener, F. J., Schultz, M. G., Gong, S., Mackenzie, I. A., Zeng, G., Hess, P., Duncan, B. N., Bergmann, D. J., Szopa, S., Jonson, J. E., Keating, T. J. and Zuber, A.: Modelling future changes in surface ozone: A parameterized approach, Atmos. Chem. Phys., 12(4), 2037–2054, doi:10.5194/acp-12-2037-2012, 2012.

de Wit, H. A., Hettelingh, J.-P. and Harmens, H.: Trends in ecosystem and health responses to long-range transported atmospheric pollutants (ICP Waters Report 125/2015). [online] Available from: https://www.unece.org/fileadmin/DAM/env/documents/2016/AIR/Publications/Trends_in_ecosystem_and_health_responses_to_long-range_transported_atmospheric_pollutants.pdf, 2015.

Wu, T., Zhang, F., Zhang, J., Jie, W., Zhang, Y., Wu, F., Li, L., Liu, X., Lu, X., Zhang, L., Wang, J. and Hu, A.: Beijing Climate Center Earth System Model version 1 (BCC-ESM1): Model Description and Evaluation, Geosci. Model Dev. Discuss., (July), 1–47, doi:10.5194/gmd-2019-172, 2019a.

Wu, T., Lu, Y., Fang, Y., Xin, X., Li, L., Li, W., Jie, W., Zhang, J., Liu, Y., Zhang, L., Zhang, F., Zhang, Y., Wu, F., Li, J., Chu, M., Wang, Z., Shi, X., Liu, X., Wei, M., Huang, A., Zhang, Y. and Liu, X.: The Beijing Climate Center Climate System Model (BCC-CSM): the main progress from CMIP5 to CMIP6, Geosci. Model Dev., 12(4), 1573–1600, doi:10.5194/gmd-12-1573-2019, 2019b.

Young, P. J., Archibald, A. T., Bowman, K. W., Lamarque, J.-F., Naik, V., Stevenson, D. S., Tilmes, S., Voulgarakis, A., Wild, O., Bergmann, D., Cameron-Smith, P., Cionni, I., Collins, W. J., Dalsøren, S. B., Doherty, R. M., Eyring, V., Faluvegi, G., Horowitz, L. W., Josse, B., Lee, Y. H., MacKenzie, I. A., Nagashima, T., Plummer, D. A., Righi, M., Rumbold, S. T., Skeie, R. B., Shindell, D. T., Strode, S. A., Sudo, K., Szopa, S. and Zeng, G.: Pre-industrial to end 21st century projections of tropospheric ozone from the Atmospheric Chemistry and Climate Model Intercomparison Project (ACCMIP), Atmos. Chem. Phys., 13(4), 2063–2090, doi:10.5194/acp-13-2063-2013, 2013.

Young, P. J., Naik, V., Fiore, A. M., Gaudel, A., Guo, J., Lin, M. Y., Neu, J. L., Parrish, D. D., Rieder, H. E., Schnell, J. L., Tilmes, S., Wild, O., Zhang, L., Ziemke, J. R., Brandt, J., Delcloo, A., Doherty, R. M., Geels, C., Hegglin, M. I., Hu, L., Im, U., Kumar, R., Luhar, A., Murray, L., Plummer, D., Rodriguez, J., Saiz-Lopez, A., Schultz, M. G., Woodhouse, M. T. and Zeng, G.: Tropospheric Ozone Assessment Report: Assessment of global-scale model performance for global and regional ozone distributions, variability, and trends, Elem Sci Anth, 6(1), 10, doi:10.1525/elementa.265, 2018.

Zhang, J., Wu, T., Shi, X., Zhang, F., Li, J., Chu, M., Liu, Q., Yan, J., Ma, Q. and Wei, M.: BCC BCC-ESM1 model output prepared for CMIP6 CMIP, , doi:10.22033/ESGF/CMIP6.1734, 2018.

Zhang, J., Wu, T., Shi, X., Zhang, F., Li, J., Chu, M., Liu, Q., Yan, J., Ma, Q. and Wei, M.: BCC BCC-ESM1 model output prepared for CMIP6 AerChemMIP, , doi:10.22033/ESGF/CMIP6.1733, 2019.